A process-based model of conifer forest structure and function with special emphasis on leaf lifespan

Colin P. Osborne and David J. Beerling

Department of Animal and Plant Sciences, University of Sheffield, Sheffield, UK

Abstract. We describe the University of Sheffield Conifer Model (USCM), a process-based approach for simulating conifer forest carbon, nitrogen, and water fluxes by up-scaling widely applicable relationships between leaf lifespan and function. The USCM is designed to predict and analyze the biogeochemistry and biophysics of conifer forests that dominated the ice-free high-latitude regions under the high pCO_2 'greenhouse' world 290 to 50 Myr ago. It will be of use in future research investigating controls on the contrasting distribution of ancient evergreen and deciduous forests between hemispheres, and their differential feedbacks on polar climate through the exchange of energy and materials with the atmosphere. Emphasis is placed on leaf lifespan because this trait can be determined from the anatomical characteristics of fossil conifer woods and influences a range of ecosystem processes. Extensive testing of simulated net primary production and partitioning, leaf area index, evapotranspiration, nitrogen uptake and land surface energy partitioning showed close agreement with observations from sites across a wide climatic gradient. This indicates the generic utility of our model, and adequate representation of the key processes involved in forest function using only information on leaf lifespan, climate, and soils.

1. Introduction

The current situation of glaciated polar regions surrounded by sparse, low-stature tundra is unusual in the geologic history of vascular land plants [*Frakes et al.*, 1992]. The plant fossil record demonstrates that tall, productive, conifer forests covered the high latitude landmasses between the Permian and the Eocene, 290 to 50 million years (Myr) ago [*Jefferson*, 1982; *Spicer and Parrish*, 1986, 1990; *Spicer and Chapman*, 1990; *Taylor et al.*, 1992]. These ancient polar forests provide tangible evidence for a major poleward advancement of the tree line, and flourished under a high pCO_2 [*Crowley and Berner*, 2001] and a warm, ice-free climate [*Frakes et al.*, 1992], despite extended periods of continuous summer daylight and winter darkness [*Read and Francis*, 1992; *Beerling and Osborne*, 2002]. One of the most intriguing features of these ecosystems was the distinctive biogeography of their leaf habit, with a mixture of evergreen and deciduous species in Arctic forests, and evergreens predominating on Antarctica [*Falcon-Lang*, 2000a,b; *Falcon-Lang and Cantrill*, 2000, 2001]. Contemporary evergreen and deciduous forests alter the seasonal course of vegetation-climate feedbacks, particularly at the regional scale [*Bonan et al.*, 1992; *Sellers et al.*, 1996; *Betts et al.*, 1997; *Levis et al.*, 1999; *Douville et al.*, 2000]. The action of forest feedbacks on climate, through changes in land surface energy, moisture and momentum fluxes, are especially strong in the mid- to high-latitude regions, and presumably operated in the distant past [*Otto-Bliesner and Upchurch*, 1997]. However, paleoclimate

modeling studies have tended to uncouple land-atmosphere energy exchanges from physiological processes and their responses to the global environment.

Just how the polar climate influenced the biogeography of these ancient forests [*Axelrod,* 1966, 1984; *Douglas and Williams*, 1982; *Creber and Chaloner*, 1985] and how, in turn, the forests affected regional climates, continues to remain uncertain. Conifer forests are optically darker than other vegetation types, allowing them to absorb more solar radiation, with a greater potential for evaporating water and heating the air and soil [*Jarvis et al*., 1976]. They are also aerodynamically rougher, enhancing the transfer of mass and energy through increased turbulence. These feedback characteristics therefore represent a 'missing link' in palaeoclimate modeling studies [*Otto-Bliesner and Upchurch*, 1997; *Beerling*, 2000], which consistently produce high-latitude winter temperatures far below freezing [*Markwick,* 1994; *Greenwood and Wing*, 1995]. This result is incompatible with corresponding biotic indicators of climate that suggest the existence of mild high-latitude winters [*e.g. Markwick,* 1994; *Greenwood and Wing*, 1995].

New techniques in paleobotany [*Falcon-Lang*, 2000a,b], and novel observations from global-scale plant physiological studies [*Reich et al.*, 1992, 1997, 1998a,b, 1999], now offer the potential to develop a new mechanistic approach for investigating these issues. In the paleobotanical realm, *Falcon-Lang* [2000a, b] has established an important quantitative technique for determining leaf lifespan from cellular analyses of fossil conifer woods. His approach utilizes the inverse correlation between growth ring markedness (defined as the percentage of late wood and decline in cell size within a given ring) and leaf lifespan across a wide range of contemporary northern and southern hemisphere conifer taxa. Initial studies on tropical (2-13 ºS) Carboniferous gymnosperm woods and high latitude (72 ºS) early-Cretaceous fossil conifer woods indicate evergreen forests in both cases, in agreement with more traditional palaeobotanical approaches [*Falcon-Lang and Cantrill*, 2001]. Interestingly, leaf retention times of the Antarctic species were estimated to be 5-13 years, values approaching the upper limit in modern conifers [*Chabot and Hicks*, 1982].

Alongside these developments in paleobotany, *Reich et al.* [1992, 1997, 1998a,b, 1999] reported, from a global set of observations, that leaf lifespan was strongly related to carbon uptake (by photosynthesis) and loss (by respiration), transpiration and nutrient content. The relationships between leaf form, function, chemistry, and longevity are remarkably robust and hold for terrestrial plants with contrasting evolutionary and climatic histories [*Reich et al.*, 1997]. In general, longer-lived leaves are mechanically tougher [*Coley*, 1988], have a lower nitrogen content, stomatal conductance, and rates of photosynthesis and respiration than their shorter-lived counterparts (Figure 1) [*Reich et al*., 1992, 1998a, b, 1999]. These traits slow ecosystem cycling of carbon and nutrients by leading to high biomass canopies with longer residence times, and by retarding rates of soil nutrient release by litter decomposition (Figure 1) [*Schlesinger*, 1997]. Collectively, the functional interactions between leaf lifespan

and key plant traits govern major components of conifer forest ecology and biogeochemistry, and offer great scope for numerically modeling these processes.

Building on this research, we describe a generic process-based model of conifer forest structure and function (University of Sheffield Conifer model, USCM), which emphasizes leaf lifespan through the fundamental relationships reported by *Reich et al.* [1992, 1998a, b, 1999]. The objective of this paper is to examine the hypothesis that a conifer model, using leaf lifespan as the driving physiological variable, can explain large-scale distribution patterns of leaf area index and net primary productivity. The work is developed with the long-term research objective of reconstructing high-latitude forests that existed 290-50 Myr ago, and their interactions with the greenhouse climate that prevailed at the time.

2. Model Description

Our model focuses on the large-scale implications of variation in leaf lifespan (Figure 1), and is designed for application at scales ranging from local to global, both in the present and geologic past. Four important aspects of forest function and their coupling are considered in relation to leaf lifespan: carbon exchange with the atmosphere, fluxes of water through the soil-plant-atmosphere continuum, limitation of growth by nitrogen, and land surface-atmosphere energy exchange (Figure 2, Table 1). Leaf lifespan is a key input to the model and is integrated so that its impacts on the carbon, nitrogen, water and energy budgets cascade to progressively larger scales (Figure 1, Table 1). Inclusion of leaf lifespan and conifer-specific environment responses provide a more direct means of scaling from fossil wood analyses [*Falcon-Lang*, 2000a,b; *Falcon-Lang and Cantrill*, 2000, 2001] than might be achieved using generic global vegetation models [e.g. *Cramer et al.,* 2001; *McGuire et al.*, 2001].

2.1. Carbon Balance

The net primary productivity of vegetation P_n is the annual balance between net canopy photosynthesis A_c and respiration R. Respiration produces the energy for two main groups of processes, and these are divided for the purposes of modeling, although they share a number of biochemical pathways [*Amthor*, 2000]: first, the maintenance of existing plant tissues via the processes of repair, turnover, acclimation and active transport R_M; secondly the growth of leaf bud, root tip and woody cambium meristems, accounting for energy expended in the nutrient uptake and transport required to supply these processes [*Lambers et al.*, 1983]. Growth respiration is expressed as the efficiency of dry matter production from fixed carbon Y_G [*Thornley*, 1970], giving

$$P_n = m_C Y_G \sum_{m=1}^{12} \left(A_c - R_M \right) , \qquad (1)$$

where A_c and R_M are calculated for each month m to give an annual net carbon balance, and m_C converts moles of fixed carbon to mass of sugars.

Net canopy photosynthesis A_c is simulated using a biochemical model of leaf photosynthesis, by treating sunlit and shaded fractions of the canopy as a 'big-leaf' [*Farquhar et al.*, 1980; *de Pury and Farquhar*, 1997]. Photosynthesis is sensitive to canopy temperature, incident solar radiation, and the diffusion of atmospheric CO_2 and O_2 into leaves. It is therefore closely coupled with both canopy energy balance and resistance to gaseous diffusion imposed by stomata (Figure 2). The impacts of leaf lifespan on these canopy processes are exerted through its relationship with photosynthetic capacity, respiration rate, stomatal conductance and the mass: area ratio (Figure 1). The control of photosynthesis and respiration by leaf lifespan operates through its relationship with nitrogen content (Figure 1).

Canopy photosynthesis is the sum of rates for sunlit A_s and shaded A_{sh} populations of leaves [*de Pury and Farquhar*, 1997], calculated for each hour of the day h, and summed for the days in each month d:

$$A_c = d \sum_{h=1}^{24} 3600\left(A_s + A_{sh}\right). \quad (2)$$

The 3600 term integrates A_c from seconds to hours. Both A_s and A_{sh} depend on the balance between respiration R_d, and CO_2 fixation, which is determined by either regeneration of the CO_2-accepting molecule Ribulose-1,5-bisphosphate (RubP) A_j, or activity of the primary carboxylating enzyme RubP carboxylase / oxygenase (Rubisco) A_v [*Farquhar et al.*, 1980]:

$$A = \min\left\{A_v, A_j\right\} - R_d \,, \quad (3)$$

where 'min' denotes 'the minimum of'. Rubisco-limited photosynthesis is governed by: the partial pressures of CO_2 and O_2 within the leaf, C_i and O_i respectively; the enzyme's temperature-sensitive affinities for these gases, K_c and K_o respectively [*Bernacchi et al.*, 2001]; and its carboxylation capacity $V_{c,max}$, such that

$$A_v = V_{c,\max} \frac{C_i - C_p}{C_i + K_c\left(1 + O_i / K_o\right)}, \quad (4)$$

where C_p is the CO_2 compensation point [*von Caemmerer*, 2000]. Regeneration of RubP in the Calvin Cycle is limited by light-dependent electron transport J, so that

$$A_j = \frac{J\left(C_i - C_p\right)}{4C_i + 8C_p}, \text{ where} \quad (5)$$

$$J = \frac{\phi Q}{\sqrt{1 + \phi^2 Q^2 / J_{\max}^{\ 2}}}. \quad (6)$$

The latter is an empirical function of the electron transport capacity J_{max}, the quantum flux Q, of photosynthetically active radiation (PAR) absorbed by canopy leaves, and the quantum efficiency of electron transport ϕ. Values of $V_{c,max}$ and J_{max} are closely coordinated [*de Pury and Farquhar*, 1997]

$$J_{\max} = 2.1 V_{c,\max} , \quad (7)$$

but each responds independently to canopy temperature [*Harley et al*., 1992; *Walcroft et al*., 1997]. In addition to CO_2, O_2 and climate data, calculation of A_c therefore requires only an estimate of Q, $V_{c,\max}$ and R_d for each of the sunlit and shaded portions of the canopy.

Canopy absorption of PAR is strongly influenced by the positioning of leaves, which are aggregated into whorls or clumps in conifers. This aggregation can be represented with a foliage-clumping index Ω (Table 2), to estimate the canopy leaf area that is effective in intercepting radiation L_e [*Chen and Black*, 1992] from the actual leaf area index L_a:

$$L_e = \frac{\Omega L_a}{\chi} . \quad (8)$$

The mean Ω for ten species (Table 2) is defined as the ratio of L_e to L_a, assessed experimentally using a combination of optical and destructive methods [*Chen*, 1996]. Vegetation cover χ allows for incomplete coverage of the land surface by trees, and is calculated following *Betts et al.* [1997]. Using L_e and χ, absorption of PAR by the whole canopy Q_c, and its sunlit Q_s and shaded Q_{sh} fractions, each may be calculated on a land area basis after *de Pury and Farquhar* [1997]:

$$Q_c = \chi \int_0^{L_e} Q_b k_{bs} (1 - \rho_b) \exp(- k_{bs} L)\, dL + \chi \int_0^{L_e} Q_d k_{ds} (1 - \rho_d) \exp(- k_{ds} L)\, dL , \quad (9)$$

$$Q_s = \chi \int_0^{L_e} Q_b k_b \alpha_p \exp(- k_b L)\, dL + \chi \int_0^{L_e} Q_d k_{ds} (1 - \rho_d) \exp\{- L(k_b + k_{ds})\}\, dL + \chi \int_0^{L_e} Q_b \left[k_{bs} (1 - \rho_b) \exp\{- L(k_b + k_{bs})\} - \alpha_p k_b \exp(- 2 k_b L) \right] dL \quad (10)$$

and $Q_{sh} = Q_c - Q_s$. (11)

The canopy extinction coefficients for beam and scattered PAR k_{bs}, diffuse and scattered PAR k_{ds}, and beam PAR k_b, vary with the solar zenith angle θ [*de Pury and Farquhar*, 1997]. Similarly, the canopy reflection coefficients for beam PAR ρ_b and diffuse PAR ρ_d depend on θ and leaf PAR absorptance α_p (Table 2) [*de Pury and Farquhar*, 1997]. We estimate the incident beam Q_b and diffuse Q_d PAR using solar geometry and the empirical formulae of *Weiss and Norman* [1985], by assuming a well-broken low cloud cover [*Lumb*, 1964].

The vertical canopy profile of leaf physiological properties is derived from the area-based decline in nitrogen content N_a with depth in the canopy, and integrated to obtain $V_{c,max}$ for

sunlit V_s and shaded V_{sh} canopy fractions [*de Pury and Farquhar*, 1997]. In a number of contrasting woody species, including conifers, the bulk of the decrease in N_a is attributable to a reduction in the leaf mass-to-area ratio, rather than any significant change in nitrogen concentration N_l [*Hollinger*, 1989; *Ellsworth and Reich*, 1993; *Rambal et al.*, 1996; *Bond et al.*, 1999]. The leaf mass-to-area ratio M declines at a constant rate with depth in the canopy (Figure 3), from a value in the uppermost leaf positions M_0 that correlates with Z_l [*Reich et al.*, 1999]:

$$M_L = M_0 - k_M L\,, \tag{12}$$

$$\log\left(1/M_0\right) = 2.43 - 0.46\log Z_l\,, \tag{13}$$

where M_L is the value of M beneath a leaf area index of L, and k_M is the rate of decrease, derived from observations of three conifer species with contrasting shade tolerance (Figure 3). Equation 12 was fitted by setting M_0 to the observed mean value of each species. The canopy profile of $V_{c,max}$ tracks M_L

$$V_{c,\max} = \sigma_v V_m \left(M_0 - k_M L\right), \tag{14}$$

where V_m is the Rubisco carboxylation capacity on a foliage mass basis, and σ_v accounts for the decline in $V_{c,max}$ with leaf age. Field evidence from a wide range of conifer species demonstrates a decline in photosynthetic capacity with leaf age, from a maximum shortly after full leaf expansion to a minimum of around zero at leaf abscission [*Reich et al*., 1995]. This decline may be mechanistically linked with seasonal variation in soil nitrogen availability [*Thornley*, 1998]. However, it occurs continuously over several growing seasons in the case of an evergreen leaf [*Reich et al*., 1995], and is poorly correlated with nitrogen in some deciduous species [*Wilson et al.*, 2000a], highlighting important uncertainty in the underlying mechanism. We therefore use the empirical factor σ_v, and integrate this important effect to the canopy scale by simulating a single cohort of leaves each year, which emerges from buds located throughout the canopy. For deciduous trees, the canopy $V_{c,max}$ declines from its maximum value to zero within a single growing season, giving:

$$\sigma_v = \frac{\left(Z_l - t\right)}{Z_l}\,, \tag{15a}$$

where t is the time elapsed since leaf budburst. The average canopy value of σ_v for evergreens must account for multiple cohorts of leaves, each separated by a year in age:

$$\sigma_v = \left(1 - \sigma_{\min}\right)\frac{\left(Z_l - t\right)}{Z_l} + \sigma_{\min}\,, \tag{15b}$$

where σ_{min} is the minimum canopy value of σ_v, immediately before the flush growth of new leaves, given by

$$\sigma_{\min} = \frac{Z_l - 12}{Z_l}. \quad (16)$$

The values of V_s and V_{sh} are obtained by integrating 14 for sunlit and shaded canopy fractions after *de Pury and Farquhar* [1997]:

$$V_c = \chi\sigma_v \int_0^{L_e} \left[V_m\left(M_0 - k_M L\right)\right] \mathrm{d}L \,, \quad (17)$$

$$V_s = \chi\sigma_v \int_0^{L_e} \left[V_m\left(M_0 - k_M L\right)\exp\left(-k_b L\right)\right] \mathrm{d}L \,, \quad (18)$$

$$V_{sh} = V_c - V_s \,. \quad (19)$$

The value of V_m is calculated from N_l (Figure 3):

$$\log V_m = 2.22 \log N_l - 3.28 \,. \quad (20)$$

The close correlation between these variables (Figure 3) was obtained using paired observations of mean photosynthesis and leaf nitrogen for eight diverse biomes [*Reich et al*., 1999], with V_m calculated following *Beerling and Quick* [1995]. Since N_l is also correlated with leaf lifespan Z_l [*Reich et al*., 1998a], canopy photosynthesis ultimately depends on this trait (Figure 1):

$$\log N_l = 1.57 - 0.34 \log Z_l \,. \quad (21)$$

Leaf respiration is sensitive to temperature and strongly inhibited by light [*Atkin et al.* 2000]. Although some evidence points to a direct repression of activity in key respiratory enzymes by elevated $p\mathrm{CO}_2$, this remains controversial, and is not considered at present [*Drake et al.*, 1999]. Leaf respiration is thus

$$R_d = r_T r_Q R_a \,, \quad (22)$$

where R_a is R_d under standard conditions of temperature and light. The response of R_d to absorbed PAR r_Q follows *Amthor* [1994], and its temperature sensitivity r_T is described by an Arrhenius response with an activation energy H_r (Table 2) [*Walcroft et al.*, 1997]. Values of R_a for sunlit and shaded portions of the canopy are obtained by substituting V_m with mass-based canopy dark respiration R_m in 17-19. The relationship between R_m and N_l is similar to the correlation between V_m and N_l (20), because the turnover of nitrogen-rich proteins such as Rubisco is metabolically expensive [*Reich et al*., 1998b; *Amthor*, 2000]. Without compelling evidence for a shift in the balance between photosynthesis and respiration with leaf lifespan [*D.S. Ellsworth,* personal communication; *Reich et al*., 1998b, 1999], we adopted a direct relationship between R_m and V_m derived from mean observations for eight diverse biomes [*Reich et al*., 1999] (Figure 3):

$$R_m = 0.022 V_m + 3.1 \,. \quad (23)$$

This method is supported by a mechanistic link between the energy requirements of Rubisco turnover and respiratory activity [*Penning de Vries*, 1975].

Maintenance respiration of non-photosynthetic organs R_M occurs largely in the roots R_r, and living cells of the sapwood R_s:

$$R_M = d\left(R_r + R_s\right). \quad (24)$$

Root respiration is sensitive to temperature and closely correlated with the nitrogen concentration in coarse N_{cr} and ephemeral N_{er} roots (Table 2), because of a tight coupling between nitrogen, protein content and metabolic activity [*Ryan et al.*, 1996]:

$$R_r = 24 \times 3600 \times r_T r_N \left[N_{er}\varphi_r + N_{cr}\left(1-\varphi_r\right)\right]W_r \times 10^{-9}, \quad (25)$$

where r_N is the sensitivity of respiration to root nitrogen content, W_r is the total root mass, and φ_r is the fraction of W_r comprised of ephemeral roots (Table 2). The temperature-sensitivity of root respiration follows an Arrhenius response (Table 2). Field evidence suggests that root respiration is negligible during the period of winter dormancy [*Striegl and Wickland*, 1998], when physiological activity approaches a minimum. We therefore consider fine root respiration to be zero during leafless periods in deciduous trees.

The maintenance respiration of sapwood is more closely related to its volume v_s than nitrogen concentration N_s [*Ryan et al.*, 1995], giving

$$R_s = r_T r_V v_s, \quad (26)$$

where r_V is the respiration rate per unit sapwood volume (Table 2). The value of v_s is estimated from tree height and the cross-sectional area of sapwood [*Osborne and Beerling*, 2002].

The growth efficiency Y_G is insensitive to environmental conditions, but differs between different plant tissue types according to their chemical composition (Table 2). It is weighted by P_n:

$$Y_G = \sum_i \left[\frac{P_i}{P_n} Y_{Gi}\right], \quad (27)$$

where the subscript i denotes leaves, roots or sapwood, for P_n or Y_G. The cost of leaf growth increases on an area basis because M rises with lifespan (13), but the mass-based Y_G remains unchanged [reviewed by *Poorter and Villar*, 1997]. Field evidence demonstrates that this occurs because a decline in energetically expensive proteins with lifespan is paralleled by a decrease in energetically cheap minerals [*Poorter and de Jong*, 1999].

2.2. Energy and Water Budgets

Net radiation at the canopy Φ_n and soil Φ_s surfaces is dissipated by latent λE, sensible H, and soil G_s heat fluxes [*Monteith and Unsworth*, 1990]

$$\Phi_n + \Phi_s = \lambda E + H + G_s . \quad (28)$$

The influx of energy to the canopy from absorbed PAR P_c and near infrared radiation (NIR) N_c is calculated using 9, with appropriate values for leaf absorptance (Table 1). Downward flux of longwave radiation from the sky L_d is an additional energy source, which varies with air and cloud temperature [*Jones*, 1992], and the cloud cover (assumed to be 50%). Longwave radiation is also emitted upward and downward L_c from the canopy, and upward from the soil L_s, tracking the temperature of each according to Stefan's Law [*Monteith and Unsworth*, 1990]. Net canopy radiation is thus

$$\Phi_n = P_c + N_c + L_d - 2L_c + L_s . \quad (29)$$

The value of Φ_s depends on PAR and NIR penetration of the canopy, and the extent to which this energy is absorbed by the soil and woody parts of trees, described by the absorptance of each, α_s and α_w, respectively:

$$\Phi_s = \alpha_s\left[\chi\left(1-\alpha_w\right)+\left(1-\chi\right)\right]\left(P_I - P_c + N_I - N_c\right) + L_c - L_s . \quad (30)$$

The soil warms during summer, and cools over the winter following observations [*Williams et al.*, 1992], and we therefore approximate G_s as 10% of Φ_s [*Clothier et al.*, 1986], as an influx in summer and efflux in winter.

Latent heat flux from a forest is comprised of transpiration by vegetation λE_t, evaporation of rainfall intercepted by the leaf canopy λE_i, and evaporation from the soil surface λE_e. These are governed by physical properties of the atmosphere and water, aerodynamic characteristics of the vegetation and stomatal conductance of the canopy [*Penman*, 1948*; Monteith*, 1965]

$$\lambda E_i = \frac{s\Phi_n + \rho_a c_p g_a D_a}{s+\gamma}, \text{ for } I > 0, \quad (31)$$

$$\lambda E_t = \frac{s\Phi_n + \rho_a c_p g_a D_a}{s+\gamma\, g_a / g_W}, \text{ for } I = 0, \quad (32)$$

$$\lambda E_e = \beta\left[\frac{s\Phi_s + \rho_a c_p g_f D_a}{s+\gamma}\right], \quad (33)$$

where I is the quantity of precipitation p intercepted by the canopy [*Woodward*, 1987] and β is the ratio of actual to potential λE_e, which increases with soil water content and wind speed [*Chanzy and Bruckler*, 1993], although the latter tends to be very low at the forest floor [*Wilson et al*., 2000b]. The aerodynamic conductance for evaporation from the forest floor

g_f [*Jones*, 1992] is estimated by assuming a roughness length of 0.01m [*Shuttleworth and Wallace*, 1985] and wind speed of 0.4 m s^{-1} at 1m above the ground [*Woodward*, 1987]. The temperature dependences of s, the rate of change of saturation vapor pressure with temperature; γ, the psychrometer constant; ρ_a, the density of dry air; and D_a are accounted for following *Jones* [1992].

Total canopy conductance to water vapor flux g_W is comprised of aerodynamic g_a and stomatal g_s conductance in series, by analogy with Ohm's Law [*Jones*, 1992]. Aerodynamic properties of the canopy depend on: tree height; the density of foliage, as represented by L_a; the characteristic dimension of leaves; and wind speed, assumed to be 20 m s^{-1} at 200m above the ground [*Shaw and Pereira*, 1982; *Jones*, 1992; *Woodward et al*., 1995]. Stomatal conductance is correlated with photosynthetic rate and leaf lifespan [*Reich et al*., 1999], and regulated in response to atmospheric CO_2 partial pressure C_a, D_a and soil water availability w_a [*Leuning*, 1995]:

$$g_{sM} = g_{cut} + \frac{36.5 - C_p}{C_a - C_p} f(D_a) f(w_a) a_1 A \,, \qquad (34)$$

where g_{sM} is g_s on a molar basis [*Woodward et al*., 1995], g_{cut} is the cuticular conductance and a_1 the stomatal sensitivity to photosynthesis (Table 2; Figure 3). The latter was fitted to paired values of A and g_s obtained from published measurements for thirteen species of conifer in four biomes (Figure 3) [*Reich et al*., 1999]. The stomatal conductance in tree canopies declines with increasing D_a, following a well-conserved relationship across a range of diverse species [*Leuning*, 1995; *Granier et al.*, 1996]. This relationship (Figure 3) was fitted to observed values of stomatal conductance [*Granier et al.*, 1996], obtained from sapflow measurements of water flux in two conifer species:

$$f(D_a) = \frac{d_1}{d_2 + D_a} \,, \qquad (35)$$

where d_1 and d_2 are fitted constants (Table 2). Chemical and hydraulic signals from the root system also induce stomatal closure in response to soil drying (Figure 3):

$$f(w_a) = 1 - s_1 \exp[s_2 w_a] + s_{\min} \,, \qquad (36)$$

where $s_{\min}$ is the minimum value of $f(w_a)$ in the field, while s_1 and s_2 are fitted constants (Table 2). The relationship describes the model of *Granier and Loustau* [1994], developed using sapflow measurements of the seasonal changes in canopy water fluxes during drought (Figure 3). Values of g_{sM} are calculated independently for sunlit and shaded populations of leaves by coupling with the photosynthesis model, and summed to obtain a whole-canopy conductance for the transpiration model.

The balance between atmospheric pCO_2, photosynthetic CO_2 demand and canopy conductance to the gas gives a value of C_i for sunlit and shaded populations of canopy leaves:

$$C_i = C_a - P\left(\frac{1.6\,A}{10^3\,g_{sM}}\right), \tag{37}$$

where P is the atmospheric pressure. Air temperature T_a and the canopy exchange of sensible heat H governs T_c in an analogous manner [*Monteith and Unsworth,* 1990]:

$$T_c = T_a + \frac{H}{\rho_a c_p g_a}, \tag{38}$$

where H is obtained by re-arranging 28

$$H = \Phi_n + \Phi_s - \lambda E - G_s. \tag{39}$$

These calculations of T_c and C_i allow the coupling of carbon, water and energy flux models following a well-established approach [*Collatz et al*., 1991]. Briefly: A_s and A_{sh} depend on C_i and T_c; g_s is sensitive to A_s and A_{sh}; Φ_n is a function of T_c; E_t is regulated by Φ_n and g_s; T_c is determined by Φ_n and E_t; and C_i by A_s, A_{sh} and g_s. *Osborne et al.* [2000] describe this canopy-scale coupling in more detail.

2.3. Nitrogen Cycling

The annual demand for nitrogen by vegetation N_p is

$$N_p = 10^3 \sum_i N_i P_i\ , \tag{40}$$

where the subscript i denotes values for leaves, roots and sapwood. Re-translocation of the nutrient from senescing leaves to the meristems N_t meets part of this demand, but the remainder must be extracted from the soil by root uptake N_u:

$$N_p \le \left(N_u + N_t\right). \tag{41}$$

Mineral nitrogen availability is a primary limitation on plant growth in natural ecosystems because soil reservoirs are highly mobile, and regulated by the biological mineralization of organic matter [*Vitousek and Howarth*, 1991]. Increasing reliance on organic nitrogen in mineral-poor soils [*Näsholm et al.*, 1998] reduces rates of plant nitrogen uptake and growth, requiring tighter symbiotic root associations with mycorrhizas [*Read*, 1990]. N_u is therefore regulated by soil availability of the nutrient, and calculated by using soil carbon s_C and nitrogen s_N as indicators of soil organic matter and plant mycorrhizal status [*Woodward and Smith*, 1994a,b]

$$N_u = \sum_{m=1}^{12}\left[120d\,\min\left\{1, s_N/600\right\}\exp\left(-8\times10^{-5}s_C\right)\right]\varphi_r W_r\ , \tag{42}$$

$$W_r = \frac{P_r}{Z_r}, \tag{43}$$

where P_r is the net annual production of fine roots, and Z_r their lifespan. We adopt the approach of *Woodward et al.* [1995] in

accounting for the temperature-limitation of N_u, and the immobilization of organic matter by freezing.

Re-translocation of nitrogen occurs principally from leaves, and this nitrogen recovery is correlated strongly with N_l in both evergreen (44a) and deciduous (44b) species [*Reich et al.*, 1992]

$$N_t = \frac{12 W_l}{Z_l}\left[0.585 N_l - 0.30\right], \tag{44a}$$

$$N_t = W_l\left[0.585 N_l - 0.30\right], \tag{44b}$$

where W_l is the total leaf mass, obtained by integrating M_L for the canopy M_c:

$$M_c = \int_0^{L_a}\left[M_0 - k_M L\right]dL\,. \tag{45}$$

Thus the dependence of N_t on Z_l may be both direct (44a) and indirect, via its relationship with M_L (13). Current evidence on the recovery of nutrients from senescent roots is conflicting [*Ferrier & Alexander*, 1991; *Gordon and Jackson*, 2000], and we have therefore adopted a conservative approach, with no significant root re-translocation [*Gordon and Jackson*, 2000].

2.4. Vegetation Structure

The leaf area index L_a is constrained by carbon, water and nitrogen. First, L_a must allow shaded leaves at the base of the canopy to maintain a positive annual carbon balance, after accounting for Y_{Gl} [*Woodward et al.*, 1995]. This carbon limitation of L_a is thus dictated by canopy light penetration, leaf photosynthetic and respiratory capacities. Secondly, L_a is regulated so that the annual water consumption by plants matches the recharge of soil water by precipitation [*Woodward*, 1987]:

$$E_{tot} \le \sum_{m=1}^{12}\left(p - I\right). \tag{46}$$

Long-lived leaves are more conservative in their water-use than short-lived leaves, having lower g_s (Figure 1), with the potential to develop larger leaf canopies given the same water availability. Finally, the nitrogen required to produce new foliage must be met by root uptake (41-43); if not, P_l is reduced and P_r increased until this condition is satisfied. As with water-use, L_a tends to increase with leaf lifespan because both N_l and the fraction of the canopy replaced each year decline with Z_l, lowering canopy nitrogen requirements. Additionally, L_a is constrained by P_n, which must be sufficient to meet P_l after deductions for roots (48). Annual leaf production P_l in evergreen (47a) and deciduous (47b) species is

$$P_l = \frac{12}{Z_l} L_a M_L\,, \tag{47a}$$

$$P_l = L_a M_L . \quad (47b)$$

An initial value for net root production P_r is set using a functional approach [*Givnish,* 1986; *Woodward and Osborne*, 2000], by correlation with annual water use by vegetation E_{tot} using global observations of a range of forest biomes [*Lee*, 1997]:

$$P_r = \frac{E_{tot}}{6.03}, \quad (48)$$

and assuming that roots turn over annually, i.e. root lifespan Z_r equals unity, in agreement with observations summarized for the world's needle-leaved temperate and boreal forests [*Vogt et al.*, 1986]. Since N_u is critically dependent on W_r (42) and therefore P_r (43), the latter must also be sufficient to meet vegetation demand for nitrogen N_p, and is increased from its initial value at the expense of P_l until 41 is satisfied. This increase in P_r relative to P_l (the ratio of root: shoot production) alters the primary limitation of vegetation structure from water supply (46 and 48) to nitrogen availability and uptake (41 and 42).

Net sapwood production P_s is the remainder of P_n (1) after the growth of roots P_r (43 and 48) and leaves P_l (47),

$$P_n = P_l + P_r + P_s , \quad (49)$$

although a minimum quantity of wood must be produced as twigs to support new foliage. If P_s cannot meet this twig production, forest growth is limited by the availability of fixed carbon, and P_l and P_r are reduced accordingly.

3. Model Tests

3.1. Leaf Area Index (L_a)

We compiled a database of observations from 23 conifer forests, encompassing a diverse set of climatic regimes and leaf lifespans (4 to 138 months, Table 3), to assess the accuracy of simulated L_a and P_n. The dataset represents a gradient from boreal conifer sites, where mean annual temperatures are extremely low and the growing season is short, through to warm sub-tropical sites in Florida with year-round warmth and high precipitation. It also includes forests in the Pacific Northwest and southern France where rainfall is highly seasonal, being greatest during the winter and limiting in the summer [*Müller*, 1982]. At each site, equilibrium model solutions were obtained using inputs of leaf lifespan for the dominant tree species, and soil carbon and nitrogen data (Table 3). To enable accurate simulations of L_a, we used site-average climatologies (1961-1990) [*New et al.*, 1999, 2000], since leaves at the majority of our test sites are retained for several years (Table 3), and canopy structure reflects the cumulative effect of interannual climatic variability.

Simulations of L_a by the USCM for 16 sites generally show close agreement with observations (Figure 4, $r^2 = 0.63$). The

model overestimates L_a for boreal forests dominated by *Pinus* species on nutrient-poor, free-draining sandy soils in Siberia and Canada (Figure 4; Table 3). Here, forest stand density is regularly thinned by wildfires, which limit aboveground biomass and cover [*Wirth et al.*, 1999]. Without an explicit consideration of disturbance regimes, we would therefore expect to overestimate L_a in these ecosystems. By contrast, we underestimate L_a for sites dominated by a mixture of *Pseudotsuga menziesii* and *Tsuga heterophylla* in the Pacific Northwest (Figure 4). Field observations reveal that foliage in these deep forest canopies is more highly aggregated than in other conifers, with measurements yielding a clumping-index Ω of 0.40, compared with the 0.55 used here (Table 2). Simulations with $\Omega = 0.40$ for these sites increase L_a in line with observations (Figure 4), markedly improving the regression between simulated and observed L_a (Figure 4, $r^2 = 0.88$). This suggests that greater accuracy in USCM simulations of L_a for the geologic past might be obtained by estimating Ω from fossil plant remains, particularly its needle-to-shoot area ratio component [*Chen*, 1996].

3.2. Net Primary Productivity (P_n)

Simulations for P_n used the same leaf lifespan and soils data as the test for L_a, but a climatology for the year matching observations. Across 19 sites, these showed a good correlation ($r^2 = 0.91$) with observations (Figure 5), with no major systematic bias apparent across geographical regions or leaf lifespan (Figure 5). Agreement between observations and predictions indicates that the USCM realistically reproduces the interspecific and geographical variation in conifer productivity using only climatic, soil and leaf lifespan information. We recognize that field observations, especially those of belowground productivity, are subject to significant uncertainty and so this test of our model is imperfect. Nevertheless, the observed errors are comparable to those of process-based vegetation models designed to predict the terrestrial biosphere response to future changes in pCO_2, climate, atmospheric nitrogen deposition and land use [*Cramer et al.*, 2001; *McGuire et al.,* 2001]. For these models, the published correlations between observed and predicted P_n are: $r^2 = 0.95$, $n = 15$ sites for the Sheffield Dynamic Global Vegetation Model described by *Woodward et al.* [1995]; $r^2 = 0.72$, $n = 19$ sites for the Integrated Biosphere Simulator, IBIS version 1.1 [*Foley et al.*, 1996]; and $r^2 = 0.74$, $n = 61$ sites for Biome3 [*Haxeltine and Prentice*, 1996].

3.3. Carbon Partitioning, Transpiration and Nitrogen Budgets

Four intensively studied reference sites in our database, indicated by asterisks in Table 3, were selected for testing plant carbon allocation between leaves, stems and roots, leaf area index (L_a), transpiration and nitrogen uptake. These represent a diversity of leaf lifespans and climatic regimes, including boreal sites in Siberia and Canada, a southern US swamp forest and a site in the maritime Pacific Northwest (Table 3). All data were extracted directly from the sources given in Table 3, except annual ecosystem evapotranspiration

which was compiled either from half-hourly average water vapor fluxes measured using eddy covariance [*Chen et al.*, 2001; *A. L. Dunn, S.C. Wofsy, M.L. Goulden and J.W. Munger, unpublished data*] or annual estimates [*Kelliher et al.*, 1997; *Liu et al*., 1998].

Simulated partitioning of P_n between leaves (P_l) and wood (P_s) closely matches observations at all four sites (Figure 6). Predictions of root production (P_r) show some discrepancies with observations for sites in Siberia and the Pacific Northwest (Figure 6). For the Siberian site, overestimation of P_r may arise because we assume a complete annual turnover, whereas observations suggest root lifespans exceeding 20 years [*Kajimoto et al.*, 1999]. In the case of the Pacific Northwest forests, P_r was determined [*Raich and Nadelhoffer*, 1989; *Runyon et al*., 1994] by correlation with aboveground litter production for other vegetation types, a procedure likely to introduce some error into the estimate.

We acknowledge that the physiological mechanisms underpinning carbon allocation in plants are inadequately understood at present [*Woodward et al.*, 1995; *Woodward and Osborne*, 2000]. However this model test, undertaken at the four reference sites, demonstrates that our scheme of medium complexity, based on the functional requirements of leaves and roots [*Givnish*, 1986], provides a realistic approximation to observations in forests (Figure 6). A similar scheme successfully describes shoot and root allocation for forests along productivity gradients at the global scale [*Friedlingstein et al.*, 1999]. We therefore regard it as adequate for our modeling purposes.

At the canopy scale, simulations of L_a for each forest type closely reproduce observations (Figure 6), supporting the general applicability of the relationships between canopy productivity and leaf area (12-13). Accurate representation of L_a in the USCM is important in simulations of vegetation-climate feedbacks in high-latitudes, because it influences albedo, surface roughness and the partitioning of energy fluxes at the land surface. Evapotranspiration is also important in this context, integrating the effects of canopy structure, climate, and stomatal physiology. For this variable, simulated values for all sites fall within the 20% range of uncertainty inherent in eddy covariance measurements (Figure 6), arising from missing data, instrument error, variation in the terrain and meteorological conditions [*Goulden et al*., 1996; *Moncrieff et al*., 1996].

Nitrogen availability for growth, the sum of root uptake and retranslocation from senescing tissues, is well described by the USCM (Figure 6), and important because it frequently limits productivity in conifer forests [*Bonan and van Cleve*, 1992; *Schulze et al.,* 1999]. Some of the small differences between predicted and observed nitrogen fluxes may be associated with the assumption of constant nitrogen concentrations for roots and sapwood (N_r and N_s, Table 2). It is possible that errors in observations, caused by the difficulty in estimating nitrogen re-translocation from long-lived foliage, also contribute to this discrepancy [*Gower et al.*, 2000].

3.4. Partitioning of Energy Fluxes

Realistic representation of energy exchange between the forested land surface and the surrounding atmosphere is an essential component of the biogeophysical effects of vegetation on climate [*Bonan et al.*, 1995], and therefore an important element of the model to examine. We tested predictions of the land surface energy balance over the boreal landscape, and its partitioning between fluxes associated with evapotranspiration (latent heat), sensible heat, net radiation and soil heat flux, with data reported from the Boreal Ecosystem-Atmosphere Study [*Sellers et al.,* 1995; *A. L. Dunn, S.C. Wofsy, M.L. Goulden and J.W. Munger,* unpublished data]. Although other sites have also been subject to similar intensive measurement campaigns, these data are not yet available. For this test, the USCM was forced with observations of monthly climate (temperature, precipitation and humidity). It reproduces with reasonable accuracy the seasonal course of net radiation, latent and sensible heat fluxes shown by field measurements for the Canadian boreal forest (Figure 7). Moreover, the magnitude of all three terms is in general agreement with observations, indicating a suitable treatment of the land surface energy balance. Since we have independently validated predictions of canopy structure and transpiration (Figure 6), this result supports our scheme for energy balance, canopy aerodynamics and conductance.

4. Model Sensitivity Analyses

4.1. Northern Hemisphere Simulations of Leaf Area Index (L_a) and Productivity (P_n)

We evaluated the effects of leaf lifespan on northern hemisphere patterns of L_a and P_n to assess the sensitivity of the USCM to large-scale variation in climate and soil properties. Analyses were restricted to the northern hemisphere because it encompasses the most extensive distributions of contemporary conifers [*Olson et al.*, 1983]. Simulations were performed with leaf lifespans of 6 months (deciduous habit) and 120 months (evergreen habit), representing the extremes shown by modern conifers (Table 3). The results are not intended to reflect actual or potential contemporary vegetation patterns, which are determined by climatic extremes and competition between life forms [*Woodward*, 1987]. Instead they allow assessment of model sensitivity for contrasting lifespans to a wider range of climate and edaphic conditions than represented by the reference sites (Table 3). We forced the model with interpolated sets of global climate observations averaged for the period 1961 – 1990 [*New et al.*, 1999, 2000], an atmospheric pCO_2 of 35 Pa and soil carbon and nitrogen contents from an interpolated global dataset [*Global Soil Data Task*, 2000].

Plate 1 displays the broad-scale geographical patterns of P_n and L_a resulting from the prescription of two leaf lifespans throughout the Northern Hemisphere. These reflect climatic variations (precipitation, humidity and land surface temperature) and differences in soil nutrient availability, and are in general agreement with the simulations of global vegetation models [*Woodward et al*., 1995; *Foley et al.*, 1996; *Cramer et al.*, 1999], indicating consistency between the alternative approaches.

Trees with short-lived leaves show greater variability in L_a than those with longer-lived leaves (Plate 1), because they have a higher nitrogen and carbon cost of annual canopy replacement (41 and 47), making L_a more sensitive to climate and soil nutrient uptake. Despite this, the deciduous habit leads to a marginally greater L_a (by 1 - 1.5 m^2 m^{-2}), by achieving higher photosynthetic rates under temperate conditions with adequate water and soil nutrients. Two exceptions to this general trend are apparent. First, in high-latitudes, where low temperatures limit soil nutrient supply and the length of the growing season. Secondly, in the dry tropics typical of modern savannahs and steppe vegetation [*Müller*, 1982], where the long leaf lifespan achieves a higher L_a than its shorter-lived counterpart because its rates of stomatal conductance to water vapor are lower (Figure 1) and water-use is more efficient.

Simulated spatial patterns of P_n for leaf lifespans of 6 and 120 months are similar and tend to track those of L_a (Plate 1). The shorter lifespan results in a higher P_n (by up to 2 t C ha^{-1} yr^{-1}) because higher leaf nitrogen contents (21) lead to higher maximum photosynthetic rates (20), when soil nitrogen content is adequate for the annual demand. As for L_a, the exception to these trends occurs in the high latitudes, but is more extensive in low latitude areas throughout equatorial South America and Africa, as well as southern and southeast Asia (Plate 1). Evergreen vegetation is more productive in these aseasonal, moist tropical regions because the capacity of deciduous trees to exploit the environment is constrained by a short leaf lifespan. All of these differences follow the well-characterized global ecological contrasts between evergreen and deciduous trees [*Chabot and Hicks*, 1982; *Schulze*, 1982; *Hollinger*, 1992], indicating that the USCM may be of use for investigating the climatic and edaphic controls on the leaf habit of modern vegetation.

4.2. Sensitivity to Atmospheric CO_2, Climate Warming and Solar Energy

Our model has been designed for analyzing polar forest biogeography and biogeochemistry between 290 and 50 Myr ago. It should therefore include appropriate sensitivity to a variety of past environmental conditions. Critical among these are CO_2, climate and solar energy, which influence plant processes from the scale of individual leaves to whole ecosystems [*Beerling,* 1994, 1997, 2000]. Long-term carbon cycle models [*Berner and Kothavala*, 2001] and isotopic evidence from fossil soils [*Ekart et al.*, 1999] indicate pCO_2 levels several times higher than current ambient during past greenhouse episodes [*Crowley and Berner*, 2001]. Additionally, many of these episodes are characterized by intense volcanic activity resulting from continental rifting. Volcanism itself exerts an influence on atmospheric CO_2, in the short-term [*McElwain et al*., 1999; *Jones and Cox*, 2001; *Beerling*, 2002], and the quality of incoming solar radiation, as seen following the ejection of aerosols by the eruptions of El Chichon in 1982 and Mount Pinatubo in 1991 [*Olmo et al.*, 1999]. Instrumental records showed attenuation of direct, and enhancement of diffuse, solar radiation, and a peak global cooling of 0.4 K after the Pinatubo eruption [*McCormick et al.*,

1995]. Coupled ocean-atmosphere climate simulations of this event, with an interactive carbon cycle, indicate an impact of the cooling on the terrestrial biosphere, with significant net uptake of carbon by ecosystems in the tropics, but no major variations in oceanic carbon cycling [*Jones and Cox*, 2001].

We therefore performed a series of model experiments assessing the sensitivity of P_n at our four reference sites (Table 3) to a rise in atmospheric pCO_2 from 30 to 100 Pa, a range representing variations over the past 100 Myr [*Ekart et al*., 1999; *Berner and Kothavala*, 2001]. At each site, three experiments were performed to simulate episodes of global warming and volcanism: 'control', using unmodified climate; 'warming', with a 4.8 K rise in mean monthly temperature; 'warming' + an 'aerosol' term, defined from observations [*Olmo et al.*, 1999] as a 10% reduction in direct and 33% enhancement of diffuse solar radiation. This change in the quality of solar radiation has little impact on total radiation, which changes by less than ± 5% depending on θ. The 4.8 K warming is equivalent to the radiative forcing effect from an increase in pCO_2 to 100 Pa, calculated after *Kothavala et al.* [1999]. Reductions in temperature following volcanic eruptions have not been investigated in this sensitivity analysis because they are within the range of uncertainty for paleotemperature proxies [*Crowley and North*, 1991].

A rise in atmospheric pCO_2 increases P_n in an asymptotic manner at all sites (Figure 8). However, the asymptote differs between sites, with stimulation of P_n between 35 and 60 Pa pCO_2 of 28% in the southern US forest, 38% in Siberia, 45% in the Pacific Northwest and 56% in Canada (Figure 8). In support of the predicted P_n increase for the southern US forest, we note that *DeLucia et al*. [1999] reported a 25 % stimulation in a young *Pinus taeda* plantation in the Duke Forest after two years' free-air CO_2 enrichment to 56 Pa. With a warming, P_n increased further for any given pCO_2 at all sites (Figure 8). As yet, no information has been reported from similar experiments with CO_2 enrichment and warming applied together, but other vegetation modeling studies support our findings for boreal conifer forests [*Beerling et al.,* 1997; *White et al.,* 2000].

In the USCM, the CO_2 response of P_n is mediated by the net effect of several interacting factors. Rising pCO_2 competitively inhibits the oxygenase activity of Rubisco and relieves substrate limitation of photosynthesis [*Drake et al.,* 1997]. The stronger increase of P_n with pCO_2 at higher temperatures results from the synergistic interaction of these environmental variables on the photosynthetic system [*Long*, 1991]. A feedback also operates between the stimulation of P_n by pCO_2 and carbon allocation to roots. As P_n increases, there is an associated rise in the demand for nitrogen, which is met by a proportional increase in root growth (42-43). This allocation of carbon to roots, away from leaves and wood, offsets the CO_2 enhancement of P_n, because of their high maintenance respiration costs and turnover.

CO_2-saturated P_n values for all but the southern US site are constrained by the mean annual temperature (Figure 9), highlighting the significance of synergism between pCO_2 and temperature. Imposition of warming in our model simulations shifts the CO_2-saturated P_n so that all follow a common trajectory given the prescribed soil characteristics, matching

experimental evidence [*Rustad et al.,* 2001]. At the southern US swamp forest site, annual demand by the deciduous canopy for nitrogen in high pCO_2 outstrips the rate of uptake from the carbon-rich soil, where the decomposition of organic matter is retarded by a high water table [*Schlesinger*, 1978]. When this constraint is alleviated, CO_2-saturated P_n rises to conform with the temperature-limited rates of other sites (Figure 9), demonstrating the importance of coupling the above- and below-ground nitrogen cycles [cf. *Bonan and van Cleve*, 1992].

The simulated effect of an increase in diffuse relative to direct radiation was typically an enhancement of P_n ('warming + aerosols', Figure 8), due to enhanced and more uniform light penetration into the leaf canopy, resulting in more efficient photosynthetic CO_2 uptake [Roderick et al., 2001]. This increase in P_n could strengthen the terrestrial carbon sink following volcanic eruptions, with an effect on the atmospheric CO_2 record [Roderick et al., 2001], and occurs in addition to the large decline in global respiration and smaller decrease in tropical gross primary production induced by surface cooling [Jones and Cox, 2001; Rustad et al., 2001]. For the Pacific Northwest site, enhancement of diffuse radiation increases L_a by 1 m^2 m^{-2} across all pCO_2 values, leading to higher maintenance respiration costs of this already deep canopy under the mild winter climate of the region, and a net decrease in P_n ('warming + aerosols', Figure 8).

At present, the simulated response of P_n to these environmental perturbations excludes any feedback between plant litter and soil nutrient status [Bonan and van Cleve, 1992], a feature shown to be important in CO_2-enrichment experiments with conifer forests [Oren et al., 2001]. Changes in P_n and leaf lifespan affect the quantity and quality of surface litter and roots, key controls over rates of nutrient cycling through their effects on soil organic matter dynamics [Raich et al., 1991; Schlesinger, 1997; Parton et al., 1998]. Leaf lifespan is strongly linked with the rate of decomposition because trees with long-lived foliage produce recalcitrant litter, slowly releasing nutrients over long periods and ultimately generating a nutrient–poor soil. Leaves with a long lifespan are well adapted for such a soil, and their persistence is encouraged via this positive feedback [Aerts, 1995]. A major future development of our model will therefore be its coupling with a model of soil carbon and nitrogen dynamics [e.g. Raich et al., 1991; Parton et al., 1998].

5. Conclusions

Ever since the important recognition, nearly a century ago, that the polar regions were once covered by forests [*Halle*, 1913, *Nathorst*, 1914; *Seward*, 1914] debate has continued regarding the nature of their interaction with climate, especially survival during the mild, dark polar winters of the Mesozoic [*Douglas and Williams*, 1982; *Chaloner and Creber*, 1989]. Furthermore, the question of how the biogeochemical and biophysical characteristics of these unusual forests influenced regional climate in an ancient high CO_2 'greenhouse' world remains uncertain. To address these issues in a predictive, quantitative manner, we designed a process-

based model of conifer function and structure, emphasizing the influence of leaf lifespan and its interactions with the environment.

Overall, a wide range of simulated vegetation properties validated well against observations from different taxonomic groups (*Abies*, *Larix*, *Picea*, *Pinus*, *Pseudotsuga*, *Taxodium*, *Tsuga*) with varying geographical ranges [*Olson et al.*, 1983], indicating adequate representation of conifer functioning. We recognize that uncertainty exists regarding whether the plant-environment relationships seen in modern conifers are applicable to those growing in the distant past. However, the discovery of general leaf trait relationships across diverse terrestrial ecosystems, for plants with different evolutionary histories [*Reich et al.*, 1997], provides the most secure basis yet for dealing with this issue.

The model can be used in a stand-alone mode to reconstruct polar forest properties at specific sites, based on leaf lifespan estimates from fossil woods [*Falcon-Lang and Cantrill*, 2000, 2001] and paleoclimatic information from climate model simulations. Some aspects of these simulations, such as P_n or the calculation of tree height from hydraulic considerations [*Osborne and Beerling*, 2002], can be compared with detailed studies of exceptionally well-preserved *in situ* fossil forests [*Francis*, 1986, 1988]. More significantly, the next stage of development will be the coupling of above- and below-ground carbon and nitrogen cycles and the production of a conifer forest dynamics scheme using the simulated structure and function of trees with different leaf lifespans [*Shugart*, 2000]. The fully coupled USCM will then allow us to resolve detailed distributions of ancient high-latitude forests, and investigate the underlying climatic and biogeochemical controls on their biogeography, as well as their influence on regional climates.

Notation

A_c net canopy photosynthesis, mol C m^{-2} $month^{-1}$.

A_j rate of CO_2 fixation permitted by RuBP-regeneration, µmol CO_2 m^{-2} s^{-1}.

A net photosynthesis, µmol CO_2 m^{-2} s^{-1}.

A_s A for the sunlit population of leaves in the canopy, µmol CO_2 m^{-2} s^{-1}.

A_{sh} A for the shaded population of leaves in the canopy, µmol CO_2 m^{-2} s^{-1}.

A_j rate of CO_2 fixation allowed by the activity of Rubisco, µmol CO_2 m^{-2} s^{-1}.

a_1 sensitivity of g_{sM} to A, mol H_2O $mmol^{-1}$ CO_2 (Table 2).

C_a atmospheric partial pressure of CO_2, Pa.

C_i partial pressure of CO_2 in leaf intercellular air spaces, Pa.

C_p CO_2 compensation point for photosynthesis, Pa.

c_p the specific heat capacity of water, 1012, J kg^{-1} K^{-1}.

D_a atmospheric vapor pressure deficit, Pa.

DM dry matter.

d number of days in the month.

d_1, d_2 empirical descriptors of the response of g_{sM} to D_a, Pa (Table 2).

E_e evaporation of water from the soil surface, mm.

E_t transpiration of water from the leaf canopy, mm.
E_{tot} annual water-use by vegetation, mm yr^{-1}.
G_s soil heat flux, W m^{-2}.
g_a canopy aerodynamic conductance to water vapor flux, m s^{-1}.
g_{cut} cuticular conductance to water vapor flux, mmol H_2O m^{-2} s^{-1}.
g_f aerodynamic conductance to water vapor flux at the forest floor, m s^{-1}.
g_s canopy stomatal conductance to water vapor flux, m s^{-1}.
g_{sM} g_s on a molar basis, mmol H_2O m^{-2} s^{-1}.
g_W total canopy conductance to water vapor flux, m s^{-1}.
H sensible heat flux, W m^{-2}.
H_r activation energy for respiration, J mol^{-1} (Table 2).
h hour of the day.
I interception of rainfall by the leaf canopy, mm.
J light-dependent rate of electron transport, µmol electrons m^{-2} s^{-1}.
J_{max} electron transport capacity, µmol electrons m^{-2} s^{-1}.
K_c Michaelis-Menton affinity of Rubisco for CO_2, Pa.
K_o Michaelis-Menton affinity of Rubisco for O_2, kPa.
k_b canopy extinction coefficient for beam PAR.
k_{bs} canopy extinction coefficient for beam and scattered PAR.
k_{ds} canopy extinction coefficient for diffuse and scattered PAR.
k_M the rate of decline in M with cumulative leaf area index (Table 2).
L leaf area index, m^2 leaf area m^{-2} ground area.
L_a actual canopy L, m^2 leaf area m^{-2} ground area.
L_c upward or downward flux of longwave radiation from the canopy, W m^{-2}.
L_d downward flux of longwave radiation from the sky, W m^{-2}.
L_e the canopy L effective in absorbing radiation, m^2 leaf area m^{-2} ground area.
L_s upward flux of longwave radiation from the soil, W m^{-2}.
M leaf mass: area ratio, g DM m^{-2}.
M_0 M in the uppermost leaves of the canopy, g DM m^{-2}.
M_c value of M for the whole leaf canopy, g DM m^{-2}.
M_L M in leaves beneath a leaf area index of L, g DM m^{-2}.
M_{min} minimum viable value of M in shaded leaves at the bottom of the canopy, g DM m^{-2} (Table 2).
m month of the year.
m_C molecular mass associated with each carbon atom in carbohydrates $[CH_2O]_n$, 30, dimensionless.
N_a area-based leaf nitrogen content, g m^{-2}.
N_c NIR absorbed by the leaf canopy, W m^{-2}.
N_{cr} coarse root nitrogen concentration, mg N g^{-1} DM (Table 2).
N_{er} ephemeral root nitrogen concentration, mg N g^{-1} DM (Table 2).
N_l leaf nitrogen concentration, mg N g^{-1} DM.
N_i nitrogen concentration in plant partition i

	(N_l, N_s, N_{cr} or N_{er}), mg N g^{-1} DM.
N_I	incident flux of NIR, W m^{-2}.
N_p	plant nitrogen demand, g N m^{-2} ground area yr^1.
N_s	sapwood nitrogen concentration, mg N g^{-1} DM (Table 2).
N_t	re-translocation of nitrogen from senescing leaves, g N m^{-2} ground area yr^{-1}.
N_u	root uptake of nitrogen from the soil, g N m^{-2} ground area yr^{-1}.
NIR	near infrared radiation.
O_i	partial pressure of O_2 within the leaf, 21 kPa.
P	atmospheric pressure, Pa.
P_c	PAR absorbed by the leaf canopy, W m^{-2}.
P_I	incident flux of PAR, W m^{-2}.
P_i	P_n partitioned to plant part i (P_l, P_s, or P_r), g DM m^{-2} yr^{-1}.
P_l	P_n partitioned to leaves, g DM m^{-2} yr^{-1}.
P_n	net primary productivity, g DM m^{-2} yr^{-1}.
P_r	P_n partitioned to roots, g DM m^{-2} yr^{-1}.
P_s	P_n partitioned to sapwood, g DM m^{-2} yr^{-1}.
p	precipitation, mm $month^{-1}$.
PAR	photosynthetically active radiation.
Q	absorption of photosynthetically active quanta, µmol quanta m^{-2} s^{-1}.
Q_c	Q for the whole canopy, µmol quanta m^{-2} ground area s^{-1}.
Q_s	Q for the sunlit population of canopy leaves, µmol quanta m^{-2} ground area s^{-1}.
Q_{sh}	Q for the shaded population of canopy leaves, µmol quanta m^{-2} ground area s^{-1}.
R_a	R_d at 293 K in the dark, µmol CO_2 m^{-2} s^{-1}.
R_d	canopy respiration rate on an area basis, excluding photorespiration, µmol CO_2 m^{-2} s^{-1}.
R_M	maintenance respiration, mol C m^{-2} $month^{-1}$.
R_m	canopy respiration rate on a mass basis, excluding photorespiration, µmol CO_2 g^{-1} s^{-1}.
R_r	root maintenance respiration rate, µmol CO_2 m^{-2} ground area s^{-1}.
R_s	sapwood maintenance respiration rate, µmol CO_2 m^{-2} ground area s^{-1}.
r_Q	sensitivity of respiration to Q, dimensionless.
r_N	sensitivity of root respiration to nitrogen, µmol CO_2 g^{-1} N s^{-1} (Table 2).
r_T	temperature sensitivity of respiration, dimensionless.
r_v	rate of sapwood respiration on a volume basis, µmol CO_2 m^{-3} s^{-1} (Table 2).
s	the rate of change in saturation vapor pressure with temperature, Pa K^{-1}.
s_C	soil nitrogen content, g N m^{-2} ground area.
s_N	soil carbon content, g C m^{-2} ground area.
$s_{\min}$	minimum relative value of g_{sM} normally occurring under drought conditions in the field, dimensionless (Table 2).
s_1, s_2	empirical descriptors of the response of g_{sM} to w_a, dimensionless (Table 2).
T_a	air temperature, K.
T_c	canopy temperature, K.
t	time since leaf budburst, months.

$V_{c,max}$ carboxylation capacity for Rubisco on an area basis, μmol CO_2 m^{-2} s^{-1}.

V_m carboxylation capacity for Rubisco on a mass basis, μmol CO_2 g^{-1} s^{-1}.

V_s $V_{c,max}$ for the sunlit population of canopy leaves, μmol CO_2 m^{-2} s^{-1}.

V_{sh} $V_{c,max}$ for the shaded population of canopy leaves, μmol CO_2 m^{-2} s^{-1}.

v_s sapwood volume, m^3 m^{-2} ground area.

W_r root biomass, g DM m^{-2}.

w_a soil water availability between the field capacity and permanent wilting point, expressed as a dimensionless fraction.

Y_G efficiency of dry matter production from fixed carbon (additional subscripts *l*, *s* or *r* denote leaves, sapwood or roots, respectively), g DM g^{-1} glucose (Table 2).

Z_l leaf lifespan, months.

Z_r root lifespan, yr.

α_p leaf NIR absorptance, dimensionless (Table 2).

α_p leaf PAR absorptance, dimensionless (Table 2).

α_s soil absorptance, 0.88, dimensionless [*Campbell and Norman*, 1998].

α_w absorptance of shortwave radiation by tree trunks and branches, 0.80, dimensionless [*Tamai et al.* 1998; *Wilson et al.*, 2000b].

β ratio of actual to potential λE_e, dimensionless.

χ fraction of the land surface covered by tree canopies, dimensionless.

Φ_n net radiation at the canopy surface, W m^{-2}.

Φ_s net radiation at the soil surface, W m^{-2}.

ϕ quantum efficiency of electron transport, 0.24, mol electrons mol^{-1} quanta [*Harley et al.*, 1992].

γ psychrometer constant, Pa K^{-1}.

φ_r fraction of W_r comprised of ephemeral roots (Table 2).

λE latent heat flux, W m^{-2}.

λE_e λE attributable to the evaporation of water from the soil surface, W m^{-2}.

λE_i λE attributable to the evaporation of rainfall wetting the canopy, W m^{-2}.

λE_t λE attributable to transpiration from the leaf canopy, W m^{-2}.

θ solar zenith angle (rad).

ρ_a the density of dry air, 1.204, kg m^{-3}.

ρ_b canopy reflection coefficient for beam PAR, dimensionless.

ρ_d canopy reflection coefficient for diffuse PAR, dimensionless.

σ_v age-related relative decline in $V_{c,max}$ and R_d, dimensionless.

σ_{min} minimum annual value of σ_v, dimensionless.

Ω foliage clumping index, dimensionless (Table 2).

Acknowledgements. We thank F.I. Woodward, R.A. Betts and V. Brovkin for their comments on the manuscript. We appreciate the assistance, helpful discussion and advice provided by D.S. Ellsworth, S.T. Gower, H. Falcon-Lang, J. Francis, M.R. Lomas, K.B. Wilson

and F.I. Woodward during model development and preparation of this manuscript. We are grateful to J. Chen (Michigan Tech University), and A.L. Dunn, S.C. Wofsy, M.L. Goulden, J.W. Munger and others (Harvard University) for access to their unpublished data and advice on its interpretation. CPO was funded through the award of a NERC research grant (GR3/11900) to DJB. DJB gratefully acknowledges funding through a Royal Society University Research Fellowship and the Leverhulme Trust.

References

Aerts, R., The advantages of being evergreen, *Trends Ecol. Evol.*, 10, 402-407, 1995.

Amthor, J. S., Scaling CO_2-photosynthesis relationships from the leaf to the canopy, *Photosyn. Res.*, 39, 321-350, 1994.

Amthor, J. S., The McCree-de Wit-Penning de Vries-Thornley respiration paradigms: 30 years later, *Ann. Bot.*, 86, 1-20, 2000.

Atkin. O. K., J. R. Evans, M. C. Ball, H. Lambers, and T. L. Pons, Leaf respiration in the light and dark. Interactions between temperature and irradiance, *Plant Physiol.*, *122,* 915-923, 2000.

Axelrod, D. I., Origin of deciduous and evergreen habits in temperate forests, *Evolution*, *20,* 1-15, 1966.

Axelrod, D. I., An interpretation of Cretaceous and Tertiary biota in polar regions, *Palaeogeogr. Palaeoclim. Palaeoecol. 45,* 105-147, 1984.

Beerling, D. J., Modelling palaeo-photosynthesis: late-Cretaceous to present, *Phil. Trans. R. Soc.*, *B346,* 421-432, 1994.

Beerling, D. J., The net primary productivity and water use efficiency of forests in the geological past, *Adv. Bot. Res.*, *26,* 193-227, 1997.

Beerling, D. J., Global terrestrial productivity in the Mesozoic era, in *Climates: past and present*, edited by M. B. Hart, pp. 17-32, Geological Society of London, Special Publication *No. 181*, 2000.

Beerling, D. J., CO_2 and the end-Triassic mass extinction, *Nature, 415*, 386-387, 2002.

Beerling, D. J., and C. P. Osborne, Physiological ecology of Mesozoic polar forests in a high CO_2 environment, *Ann. Bot., 89*, 329-339, 2002.

Beerling, D. J., and W. P. Quick, A new technique for estimating rates of carboxylation and electron transport in leaves of C_3 plants for use in dynamic global vegetation models, *Global Change Biol.*, *1,* 289-294, 1995.

Beerling, D. J., F. I. Woodward, M. Lomas, and A. J. Jenkins, Testing the responses of dynamic global vegetation model to environmental change: a comparison of observations and predictions, *Global Ecol. Biogeogr., 6,* 439-450, 1997.

Bernacchi, C. J., E. L. Singsaas, C. Pimentel, A. R. Portis, and S. P. Long, Improved temperature response functions for models of Rubisco-limited photosynthesis, *Plant Cell Environ.*, *24,* 253-259, 2001.

Berner, R. A., and Z. Kothavala, GEOCARB III: a revised model of atmospheric CO_2 over Phanerozoic time, *Am. J. Sci.*, *301,* 182-204, 2001.

Betts, R. A., P. M. Cox, S. E. Lee, and F. I. Woodward, 1997, Contrasting physiological and structural vegetation feedbacks in climate change simulations, *Nature*, *387,* 796-799, 1997.

Bonan, G. B., F. S. Chapin, S. L. Thompson, Boreal forest and tundra ecosystems as components of the climate system, *Climatic Change, 29,* 145-167, 1995.

Bonan, G. B., D. Pollard, and S. L. Thompson, Effects of boreal forest vegetation on global climate, *Nature*, *359,* 716-718, 1992.

Bonan, G. B., K. Van Cleve, Soil-temperature, nitrogen mineralization, and carbon source sink relationships in boreal forests, *Can. J. For. Res. 22,* 629-639, 1992.

Bond, B. J., B. T. Farnsworth, R. A. Coulombe, and W. E. Winner, Foliage physiology and biochemistry in response to light gradients in conifers with varying shade tolerance, *Oecologia*, *120,* 183-190, 1999.

Bruniquel-Pinel, V., and J. P. Gastellu-Etchegorry, Sensitivity of texture of high resolution images of forest to biophysical and acquisition parameters, *Remote Sens. Environ., 65*, 61-85, 1998.

Campbell, G. S., and J. M. Norman, *An Introduction to Environmental Biophysics*, 2nd ed., 286 pp., Springer, New York, 1998.

Carey, E. V., R. M. Callaway, and E. H. DeLucia, Stem respiration of Ponderosa Pines grown in contrasting climates: implications for global climate change, *Oecologia*, *111,* 19-25, 1997.

Chabot, B. F., and D. J. Hicks, The ecology of leaf life spans, *Ann. Rev. Ecol. Syst.*, 13, 229-*259,* 1982.

Chaloner, W. G., and G. T. Creber, The phenomenon of forest growth in Antarctica: a review, in *Origins and Evolution of the Antarctic Biota*, edited by J. A. Crame, pp. 85-88, Geological Society Special Publication No. 47, London, 1989.

Chanzy, A., and L. Bruckler, Significance of soil surface moisture with respect to daily bare soil evaporation, *Water Res. Res.*, *29,* 1113-1125, 1993.

Chen, J. M., Optically-based methods for measuring seasonal variation of leaf area index in boreal conifer stands, *Ag. For. Met.*, *80*, 135-163, 1996.

Chen, J. M., and T. A. Black, Measuring leaf area index of plant canopies with branch architecture, *Ag. For. Met.*, *57,* 1-12, 1991.

Chen, J. M., and T. A. Black, Foliage area and architecture of plant canopies from sunfleck size distributions, *Ag. For. Met.*, *60,* 249-266, 1992.

Chen, J. M., T. A. Black, and R. S. Adams, Evaluation of hemispherical photography for determining plant area index and geometry of a forest stand, *Ag. For. Met., 56,* 129-143, 1991.

Chen, J., K. T. Paw U., T. Suchanek, S. Ustin, X. Wang, T. Hsiao, M. Falk, R. Shaw, K. D. Brosofske, R. Bi, and T. King, Energy budget and fluxes of CO_2 and H_2O of a 20, 40, and 500 year-old Douglas-fir forest, *Ecosystems (Special Issue)*, in press, 2001.

Chung, H. H., and R. L. Barnes, Photosynthetic allocation in *Pinus taeda*. I. Substrate requirements for synthesis of shoot biomass, *Can. J. For. Res., 7*, 106-111, 1977.

Clothier, B. E., K. L. Clawson, P. J. Pinter, M. S. Moran, R. J. Reginato, and R. D. Jackson, Estimation of soil heat flux from net radiation during the growth of Alfalfa, *Ag. For. Met.*, *37,* 319-329, 1986.

Coley, P. D., Effects of plant growth rate and leaf lifetime on the amount and type of anti-herbivore defence, *Oecologia*, *74,* 531-536, 1988.

Collatz G. J., J. T. Ball, C. Grivet, and J. A. Berry, Physiological and environmental regulation of stomatal conductance, photosynthesis and transpiration - a model that includes a laminar boundary layer. *Ag. For. Met.*, *54,* 107-136, 1991.

Connor, W. H., and J. W. Day, Productivity and composition of a baldcypress-water tupelo site and a bottomland hardwood site in a Louisiana swamp, *Am. J. Bot.*, *63,* 1354-1364, 1976.

Cramer W., D. W. Kicklighter, A. Bondeau, B. Moore, G. Churkina, B. Nemry, A. Ruimy, A. L. Schloss, and the participants of the Potsdam NPP model intercomparison, Comparing global models of terrestrial net primary productivity (NPP): overview and key results. *Global Change Biol.*, *5 (Suppl. 1)*, 1-15, 1999.

Cramer, W., A. Bondeau, F. I. Woodward, I. C. Prentice, R. A. Betts, V. Brovkin, P. M. Cox, V. Fisher, J. A. Foley, A. D. Friend, C. Kucharik, M. R. Lomas, N. Ramankutty, S. Sitch, B. Smith, A. White, and C. Young-Molling, Global response of terrestrial ecosystem structure and function to CO_2 and climate change: results from six dynamic global vegetation models, *Global Change Biol.*, *7,* 357-373, 2001.

Creber, G. T., and W. G. Chaloner, Tree growth in the Mesozoic and early Tertiary and the reconstruction of palaeoclimates, *Palaeogeogr. Palaeoclim. Palaeoecol.*, *52,* 35-60, 1985.

Crowley, T. J., and R. A. Berner, CO_2 and climate change, *Science*, *292,* 870-872, 2001.

Crowley, T. J., and G. R. North, *Paleoclimatology*, 339 pp., Oxford University Press, New York, 1991.

DeLucia, E.H., J.G. Hamilton, S.L. Naidu *et al.*, Net primary production of a forest ecosystem with experimental CO2 enrichment, *Science*, *284,* 1177-1179, 1999.

de Pury, D. G. G., and G. D. Farquhar, Simple scaling of photosynthesis from leaves to canopies without the errors of big-leaf models, *Plant Cell Environ.*, *20*, 537-557, 1997.

Douglas, J. G., and G. E. Williams, Southern polar forests: the early Cretaceous floras of Victoria and their palaeoclimatic significance, *Palaeogeogr. Palaeoclim. Palaeoecol.*, *39*, 171-185, 1982.

Douville, H., S. Planton, J.-F. Royer, D. B. Stephenson, S. Tyeca, L. Kergoat, S. Lafont, and R. A. Betts, Importance of vegetation feedbacks in doubled-CO_2 climate experiments, *J. Geophys. Res.*, *105*, D14841-D14861, 2000.

Drake, B. G., J. Azcon-Bieto, J. Berry, J. Bunce, P. Dijkstra, J. Farrar, R. M. Gifford, M. A. Gonzalez-Meler, G. Kock, H. Lambers, J. Siedow, and S. Wullschleger, Does elevated atmospheric CO_2 concentration inhibit mitochondrial respiration in green plants? *Plant Cell Environ.*, *22*, 649-657, 1999.

Drake, B. G., M. A. Gonzàlez-Meler, and S. P. Long, More efficient plants: a consequence of rising atmospheric CO_2? *Ann. Rev. Plant Physiol. Plant Mol. Biol.*, *48*, 607-637, 1997.

Dunn, A. L., S. C. Wofsy, M. L. Goulden, J. W. Munger, and others, BOREAS CO_2 flux, temperature, and meteorological data, available from http://www-as.harvard.edu/data/data.html

Ekart, D. D., T. E. Cerling, I. P. Montanez, and N. Tabor, A 400 million year carbon isotope record of pedogenic carbonate: implications for atmospheric carbon dioxide, *Am. J. Sci.*, *299*, 805-827, 1999.

Ellsworth, D. S., and P. B. Reich, Canopy structure and vertical patterns of photosynthesis and related leaf traits in a deciduous forest, *Oecologia*, *96*, 169-178, 1993.

Falcon-Lang, H. J., A method to distinguish between woods produced by evergreen and deciduous coniferopsids on the basis of growth ring anatomy: a new palaeoecological tool, *Palaeontology*, *43*, 785-793, 2000a.

Falcon-Lang, H. J., The relationship between leaf longevity and growth ring markedness in modern conifer woods and its implications for palaeoclimatic studies, *Palaeogeogr. Palaeoclim. Palaeoecol.*, *160*, 317-328, 2000b.

Falcon-Lang, H. J., and D. J. Cantrill, Cretaceous (Late Albian) coniferales of Alexander Island, Antarctica. l: wood taxonomy: a quantitative approach. *Rev. Pal. Pal.*, *111*, 1-17, 2000.

Falcon-Lang, H. J., and D. J. Cantrill, Leaf phenology of some mid-Cretaceous polar forests, Alexander Island, Antarctica, *Geol. Mag.*, *138*, 39-52, 2001.

Farquhar, G. D., S. von Caemmerer, and J. A. Berry, A biochemical model of photosynthetic CO_2 assimilation in leaves of C_3 species, *Planta*, *149*, 78-90, 1980.

Fassnacht, K. S., S. T. Gower, J. M. Norman, and R. E. McMurtrie, A comparison of optical and direct methods for estimating foliage surface area index in forests, *Ag. For. Met., 71*, 183-207, 1994.

Ferrier, R. C., and I. J. Alexander, Internal redistribution of N in Sitka spruce seedlings with partially droughted root systems. *Forest Science*, *37*, 860-870, 1991.

Foley, J. A., I. C. Prentice, N. Ramankutty, S. Levis, D. Pollard, S. Sitch, and A. Haxeltine, An integrated biosphere model of land surface processes, terrestrial carbon balance, and vegetation dynamics, *Global Biogeochem. Cycles*, *10*, 603-628, 1996.

Frakes, L. A., J. Francis, and J. I. Syktus, *Climate Modes of the Phanerozoic*, Cambridge University Press, Cambridge, 1992.

Francis, J. E., Growth rings in Cretaceous and Tertiary wood from Antarctica and their paleoclimatic implications, *Palaeontology, 26*, 665-684, 1986.

Francis, J. E., A 50-million-year-old fossil forest From Strathcona Fiord, Ellesmere Island, Arctic Canada - evidence for a warm polar climate, *Arctic*, *41*, 314-318, 1988.

Friedlingstein, P., G. Joel, C. B. Field, and I. Y. Fung, Toward an allocation scheme for global terrestrial carbon models, *Global Change Biol., 5,* 755-770, 1999.

Gates, D. M., *Biophysical Ecology*. Springer-Verlag, New York, 1979.

Gholz, H. L., Environmental limitations on aboveground net primary production, leaf area, and biomass in vegetation zones of the Pacific Northwest, *Ecology*, *63*, 469-481, 1982.

Givnish, T. J., Optimal stomatal conductance, allocation of energy between leaves and roots, and the marginal cost of transpiration, in *On the Economy of Plant Form and Function*, edited by T. J.

Givnish, pp. 171-213, Cambridge University Press, Cambridge, 1986.
Global Soil Data Task, *Global Soil Data Products CD-ROM (IGBP-DIS). International Geosphere-Biosphere Programme – Data and Information Services*. Available online at [http://www.daac.ornl.gov/] from the ORNL Distributed Active Archive Center, Oak Ridge National Laboratory, Oak Ridge, Tennessee, USA, 2000.
Gordon, W. S., and R. B. Jackson, Nutrient concentrations in fine roots, *Ecology*, *81*, 275-280, 2000.
Goulden, M. L., J. W. Munger, S.-M. Fan, B. C. Daube, and S. C. Wofsy, Measurements of carbon sequestration by long-term eddy covariance: methods and a critical evaluation of accuracy, *Global Change Biol.*, *2*, 169-182, 1996.
Gower, S. T., A. Hunter, J. Campbell, J. Vogel, H. Veldhuis, J. Harden, S. Trumbore, J. M. Norman, and C. J. Kucharik, Nutrient dynamics of the southern and northern BOREAS boreal forests, *Ecoscience*, *7*, 481-490, 2000.
Gower, S. T., J. G. Vogel, J. M. Norman, C. J. Kucharik, S. J. Steele, and T. K. Stow, Carbon distribution and aboveground net primary production in aspen, jack pine, and black spruce stands in Saskatchewan and Manitoba, Canada, *J. Geophys. Res.*, *102*, D29029-29041, 1997.
Granier, A., P. Biron, N. Bréda, J.-Y. Pontallier, and B. Saugier, Transpiration of trees and forest stands: short and long-term monitoring using sapflow methods, *Global Change Biol.*, *2*, 265-274, 1996.
Granier, A., and D. Loustau, Measuring and modelling the transpiration of a maritime pine canopy from sap-flow data, *Ag. For. Met.*, *71*, 61-81, 1994.
Greenwood, D.L. and S.L. Wing, Eocene continental climates and latitudinal temperature gradients, *Geology, 23,* 1044-1048, 1995.
Grier, C. C., and R. S. Logan, Old-growth *Pseudotsuga menziesii* communities of a western Oregon watershed: biomass distribution and production budgets, *Ecol. Mon.*, *47*, 373-400, 1977.
Halle, T. G., The Mesozoic flora of Graham Land. *Wissenschaftliche Ergebnisse der Schwedischen Südpolar-Expedition 1901-03*. Bd. III, Lief. 14, 123 pp., Taf. 1-9, 1913.
Harley, P. C., R. B. Thomas, J. F. Reynolds, and B. R. Strain, Modelling photosynthesis of cotton grown in elevated CO_2, *Plant Cell Environ.*, *15*, 271-282, 1992.
Haxeltine, A., and I. C. Prentice, BIOME3: An equilibrium terrestrial biosphere model based on ecophysiological constraints, resource availability, and competition among plant functional types, *Global Biogeochem. Cycles*, *10*, 693-709, 1996.
Hollinger, D. Y., Canopy organization and foliage photosynthetic capacity in a broad-leaved evergreen montaine forest, *Func. Ecol.*, *3*, 53-62, 1989.
Hollinger, D. Y., Leaf and simulated whole-canopy photosynthesis in two co-occurring tree species, *Ecology*, *73*, 1-14, 1992.
Jarvis, P. G., G. B. James, and J. J. Landsberg, Coniferous forest, in *Vegetation and the Atmosphere*, edited by J. L. Monteith, pp. 171-240, Academic Press, London, 1976.
Jefferson, T. H., Fossil forests from the Lower Cretaceous of Alexander Island, Antarctica, *Palaeontology*, *25*, 681-708, 1982.
Jones, C. D., and P. M. Cox, Modeling the volcanic signal in the atmospheric CO_2 record, *Global Biogeochem. Cycles*, *15*, 453-465, 2001.
Jones, H. G., *Plants and Microclimate*, 2nd ed., 428 pp., Cambridge University Press, Cambridge, 1992.
Kajimoto, T., Y. Matsuura, M. A. Sofronov, A. V. Volokitina, S. Mori, A. Osawa, and A. P. Abaimov, Above- and belowground biomass and net primary productivity of a *Larix gmelinii* stand near Tura, central Siberia, *Tree Physiol.*, *19*, 815-822, 1999.
Katul, G., C.-I. Hsieh, D. Bowling, K. Clark, N. Shurpali, A. Turnipseed, J. Albertson, K. Tu, D. Hollinger, B. Evans, B. Offerle, D. Anderson, D. Ellsworth, C. Vogel, and R. Oren, Spatial variability of turbulent fluxes in the roughness sublayer of an even-aged pine forest, *Bound.-Layer Met., 93*, 1-28, 1999.
Kelliher, F. M., D. Y. Hollinger, E.-D. Schulze, N. N. Vygodskaya, J. N. Byers, J. E. Hunt, T. M. McSeveny, I. Milukova, A.

Sogatchev, A. Varlargin, W. Ziegler, A. Arneth, and G. Bauer, Evaporation from an eastern Siberian larch forest, *Ag. For. Met.*, *85*, 135-147, 1997.
Kinerson, R. S., C. W. Ralston and C. G. Wells, Carbon cycling in a loblolly pine plantation, *Oecologia*, *29*, 11-10, 1977.
Körner, C., Leaf diffusive conductances in the major vegetation types of the globe, in *Ecophysiology of Photosynthesis*, edited by E. D. Schulze and M. M. Caldwell, pp. 463-490, Springer-Verlag, Berlin, 1994.
Kothavala, Z., R. J. Oglesby, B. Saltzman, Sensitivity of equilibrium surface temperature of CCM3 to systematic changes in atmospheric CO_2, *Geophys. Res. Lett., 26,* 209-212, 1999.
Lambers, H., R. K. Szaniawski, and R. de Visser, Respiration for growth, maintenance and ion uptake. An evaluation of concepts, methods, values and their significance, *Physiol. Plant.*, *58*, 556-563, 1983.
Lee, S.E., *Modelling interactions between climate and global vegetation in response to climate change*, Ph.D. thesis, Univ. Sheffield, UK, 1997.
Levis S, J.A. Foley, and D. Pollard, Potential high-latitude vegetation feedbacks on CO_2-induced climate change, *Geophys. Res. Lett.*, *26,* 747-750, 1999.
Leuning, R., A critical appraisal of a combined stomatal-photosynthesis model for C_3 plants, *Plant Cell Environ.*, *18*, 339-355, 1995.
Liu, S., H. Riekerk, and H. L. Gholz, Simulation of evapotranspiration from Florida pine flatwoods, *Ecol. Mod.*, *114*, 19-34, 1998.
Long, S. P., Modification of the response of photosynthetic productivity to rising temperature by atmospheric CO_2 concentrations: Has its importance been underestimated? *Plant Cell Environ.*, *14*, 729-739, 1991.
Lumb, F. E., The influence of cloud on hourly amounts of total solar radiation at the sea surface, *Q. J. Roy. Met. Soc.*, *90*, 43-56, 1964.
Markwick, P.J., 'Equability', continentality and Tertiary 'climate': the crocodilian perspective, *Geology, 22,* 613-616, 1994.
McCormick, M., L. Thomason, and C. Trepte, Atmospheric effects of the Mount Pinatubo eruption, *Nature, 373, 399-404,* 1995.
McElwain J. C., D. J. Beerling, and F. I. Woodward, Fossil plants and global warming at the Triassic-Jurassic boundary, *Science*, *285***,** 1386-1390, 1999.
McGuire, A. D., J. M. Melillo, L. A. Joyce, D. W. Kicklighter, A. L. Grace, B. Moore, and C. J. Vorosmarty, Interactions between carbon and nitrogen dynamics in estimating net primary productivity for potential vegetation in North America, *Global Biogeochem. Cycles*, *6*, 101-124, 1992.
McGuire, A. D., S. Sitch, J. S. Clein, R. Dargaville, G. Esser, J. Foley, M. Heimann, F. Joos, J. Kaplan, D. W. Kicklighter, R. A. Meier, J. M. Melillo, B. Moore III, I. C. Prentice, N. Ramankutty, T. Reichenau, A. Schloss, H. Tian, L. J. Williams, and U. Wittenberg, Carbon balance of the terrestrial biosphere in the twentieth century: analyses of CO_2, climate and land use effects with four process-based ecosystem models, *Global Biogeochem. Cycles*, *15*, 183-206, 2001.
Megonigal, J. P., and F. P. Day, Organic matter dynamics in four seasonally flooded forest communities of the Dismal Swamp, *Am. J. Bot.*, *75*, 1334-1343, 1988.
Moncrieff, J. B., Y. Malhi, and R. Leuning, The propagation of errors in long-term measurements of land-atmosphere fluxes of carbon and water, *Global Change Biol.*, *2*, 231-240, 1996.
Monteith, J. L., Evaporation and environment, in *The State and Movement of Water on Living Organisms*, edited by C. E. Fogg, pp. 205-234, Cambridge University Press, Cambridge, 1965.
Monteith, J. L., and M. Unsworth, *Principles of Environmental Physics*, 291 pp., Edward Arnold, London, 1990.
Murty, D., R. E. McMurtrie, and M. G. Ryan, Declining forest productivity in aging forest stands: a modeling analysis of alternative hypotheses, *Tree Physiol.*, *16*, 187-200, 1996.
Müller, M. J. *Selected Climatic data for a Global Set of Standard Stations for Vegetation Science*, 305 pp., Dr. W. Junk, Norwell, Mass., 1982.

Näsholm, T., A. Ekblad, A. Nordin, R. Giesler, M. Högberg, and P. Högberg, Boreal forest plants take up organic nitrogen, *Nature, 392,* 914-916, 1998.

Nathorst, A. G., Nachträge zur Pälaozoischen Flora Spitzbergens. *Zur Fossilen Flora der Polarländer*. Teil I. Lief. IV. Stockholm, 1914.

New, M., M. Hulme, and P. Jones, Representing twentieth-century space-time climate variability. Part I: Development of a 1961-1990 mean monthly terrestrial climatology, *J. Clim.*, *12*, 829-856, 1999.

New, M., M. Hulme, and P. Jones, Representing twentieth-century space-time climate variability. Part II: Development of 1901-1996 monthly grids of terrestrial surface climate, *J. Clim.*, *13*, 2217-2238, 2000.

Olmo, F. J., J. Tovar, L. Alados-Arboledas, O. Okulov, and H. O. Ohvril, A comparison of ground level solar radiative effects of recent volcanic eruptions, *Atmos. Environ.*, *33*, 4589-4596, 1999.

Oren, R., D. S. Ellsworth, K. H. Johnsen, N. Phillips, B. E. Ewers, C. Maier, K. V. R. Schäfer, H. McCarthy, G. Hendrey, S. G. McNulty, and G. G. Katul, Soil fertility limits carbon sequestration by forest ecosystems in a CO_2-enriched atmosphere, *Nature*, *411,* 469-472, 2001.

Olson, J. S., J. A. Watts, and L. J. Allison, *Carbon in Live Vegetation of Major World Ecosystems*, 164 pp., ORNL-5862, Environmental Sciences Division Publication No. 1997, Oak Ridge National Laboratory, Oak Ridge, Tennessee, 1983.

Osborne, C. P., and D. J. Beerling, Sensitivity of tree growth to a high CO_2 environment – consequences for interpreting the characteristics of fossil woods from ancient 'greenhouse' worlds. *Palaeogeogr. Palaeoclim. Palaeoecol.*, in press, 2002.

Osborne, C. P., P. L. Mitchell, J. E. Sheehy, and F. I. Woodward, Modelling the recent historical impacts of atmospheric CO_2 and climate change on Mediterranean vegetation. *Global Change Biol.*, *6*, 445-458, 2000.

Otto-Bliesner, B. L., and G. R. Upchurch, Vegetation-induced warming of high latitudes during the latest Cretaceous, *Nature*, *385*, 804-807, 1997.

Parton, W. J., M. Hartman, D. S. Ojima, and D. S. Schimel, DAYCENT and its land surface submodel: description and testing, *Global Plan. Change*, *19*, 35-48, 1998.

Penman, H. L., Natural evaporation from open water, bare soil and grass, *Proc. R. Soc. Lond.*, *A193*, 120-145, 1948.

Penning de Vries, F. W. T., The cost of maintenance processes in plant cells, *Ann. Bot.*, *39*, 77-92, 1975.

Poorter, H., and R. de Jong, A comparison of specific leaf area, chemical composition and leaf construction costs of field plants from 15 habitats differing in productivity, *New Phytol.*, *143*, 163-176, 1999.

Poorter, H., and R. Villar, The fate of acquired carbon in plants: chemical composition and construction costs, in *Plant Resource Allocation*, edited by F. A. Bazzaz and J. Grace, pp. 39-72, Academic Press, San Diego, 1997.

Raich J. W., and K. J. Nadelhoffer, Belowground carbon allocation in forest ecosystems: global trends, *Ecology*, *70*, 1346-1354, 1989.

Raich, J. W., E. B. Rastetter, J. M. Melillo, D. W. Kicklighter, P. A. Steudler, B. J. Peterson, A. L. Grace, B. Moore III, and C. J. Vörösmarty, Potential net primary productivity in South America: application of a global model, *Ecol. Applic.*, *1*, 399-429, 1991.

Rambal S., C. Damesin, R. Joffre, M. Méthy, and D. Lo Seen, Optimization of carbon gain in canopies of Mediterranean evergreen oaks, *Ann. Sci. For.*, *53*, 547-560, 1996.

Rapp, M., and A. Cabanettes, Biomass and productivity of a *Pinus pinea* L. stand, in *Components of Productivity of Mediterranean-Climate Regions – Basic and Applied Aspects*, edited by N. S. Margaris and H. A. Mooney, pp. 131-134, Dr W. Junk Publishers, The Hague, 1981.

Read, D.J., Mycorrhizas in ecosystems, *Experientia, 47,* 376-391, 1990.

Read, J., and J. Francis, Responses of some Southern Hemisphere tree species to a prolonged dark period and their implications for

high-latitude Cretaceous and Tertiary floras, *Palaeogeogr. Palaeoclim. Palaeoecol.*, *99*, 271-290, 1992.

Reich, P. B., D. S. Ellsworth, and M. B. Walters, Leaf structure (specific leaf area) modulates photosynthesis-nitrogen relations: evidence from within and across species and functional groups, *Func. Ecol.*, *12*, 948-958, 1998a.

Reich, P. R., D. S. Ellsworth, M. B. Walters, J. M. Vose, C. Gresham, J. C. Volin, and W. D. Bowman, Generality of leaf trait relationships: a test across six biomes. *Ecology*, *80*, 1955-1969, 1999.

Reich, P. B., T. Koike, S. T. Gower, and A. W. Schoettle, Causes and consequences of variation in conifer leaf life-span, in *Ecophysiology of Coniferous Forests*, edited by W. K. Smith and T. M. Hinckley, pp. 225-254, Academic Press, San Diego, 1995.

Reich, P. B., M. B. Walters, and D. S. Ellsworth, Leaf life-span in relation to leaf, plant, and stand characteristics among diverse ecosystems, *Ecol. Mon.*, *62*, 365-392, 1992.

Reich, P. B., M. B. Walters, and D S. Ellsworth, From tropics to tundra: global convergence in plant functioning, *Proc. Nat. Acad. Sci. USA*, *94*, 13730-13734, 1997.

Reich, P. B., M. B. Walters, D. S. Ellsworth, J. M. Vose, J. C. Volin, C. Gresham, and W. D. Bowman, Relationships of leaf dark respiration to leaf nitrogen, specific leaf area and leaf life-span: a test across biomes and functional groups, *Oecologia, 114,* 471-482, 1998b.

Roderick, M. L., G. D. Farquhar, S. L. Berry, and I. R. Noble, On the direct effect of clouds and atmospheric particles on the productivity and structure of vegetation, *Oecologia, 129,* 21-30, 2001.

Runyon, J., R. H. Waring, S. N. Goward, and J. M. Welles, Environmental limits on net primary production and light-use efficiency across the Oregon transect, *Ecol. Applic.*, *4*, 226-237, 1994.

Rustad, L. E., J. L. Campbell, G. M. Marion, R. J. Norby, M. J. Mitchell, A. E. Hartley, J. H. C. Cornelissen, J. Gurevitch, and GCTE-NEWS, A meta-analysis of the response of soil respiration, net nitrogen mineralization, and aboveground plant growth to experimental ecosystem warming, *Oecologia, 126,* 543-562, 2001.

Ryan, M. G., Effects of climate change on plant respiration, *Ecol. Applic.*, *1,* 157-167, 1991.

Ryan, M. G., S. T. Gower, R. M. Hubbard, R. H. Waring, H. L. Gholz, W. P. Cropper, and S. W. Running, Woody tissue maintenance respiration of four conifers in contrasting climates, *Oecologia*, *101*, 133-140, 1995.

Ryan, M. G., R. M. Hubbard, S. Pongracic, R. J. Raison, and R. E. McMurtrie, Foliage, fine-root, woody-tissue and stand respiration in *Pinus radiata* in relation to nitrogen status, *Tree Physiol.*, *16*, 333-343, 1996.

Schiller, G., and Y. Cohen, Water regime of a pine forest under a Mediterranean climate, *Ag. For. Met., 74*, 181-193, 1995.

Schlesinger, W. H., Community structure, dynamics and nutrient cycling in the Okefenokee cypress swamp-forest, *Ecol. Mon.*, *48*, 43-65, 1978.

Schlesinger, W. H., *Biogeochemistry. An analysis of global change.* 2nd ed., 588 pp., Academic Press, San Diego, 1997.

Schulze, E.-D., Plant life forms and their carbon, water and nutrient relations, in *Physiological Plant Ecology III. Water Relations and Carbon Assimilation*, edited by O. L. Lange, P. S. Nobel, C. B. Osmond, and H. Ziegler, pp. 615-676, Springer-Verlag, Berlin-Heidelberg, 1982.

Schulze, E.-D., W. Schulze, F. M. Kelliher, N. N. Vygodskaya, W. Ziegler, K. I. Kobak, H. Koch, A. Arneth, W. A. Kusnetsova, A. Sogatchev, A. Issajev, G. Bauer, and D. Y. Hollinger, Aboveground biomass and nitrogen nutrition in a chronosequence of pristine Dahurian *Larix* stands in eastern Siberia, *Can. J. For. Res.*, *25*, 943-960, 1995.

Schulze, E.-D., J. Lloyd, F. M. Kelliher, C. Wirth, C. Rebmann, B. Lühker, M. Mund, A. Knohl, I. M. Milyukova, W. Schulze, W. Ziegler, A. B. Varlagin, A. F. Sogatchev, R. Valentini, S. Dore, S. Grigoriev, O. Kolle, M. I. Panfyorov, N. Tchebakova, and N. N. Vygodskaya, Productivity of forests in the Eurosiberian boreal

region and their potential to act as a carbon sink – a synthesis, *Global Change Biol.*, *5*, 703-722, 1999.
Sellers, P. *et al*., The Boreal Ecosystem-Atmosphere Study (BOREAS): an overview and early results from the 1994 field year, *Bull. Am. Met. Soc., 76*, 1549-1577, 1995.
Sellers, P. J., L. Bounoua, G. J. Collatz, D. A. Randall, D. A. Dazlich, S. O. Los, J. A. Berry, I. Fung, C. J. Tucker, C. B. Field, and T. G. Jensen, Comparison of radiative and physiological effects of doubled atmospheric CO_2 on climate, *Science, 271*, 1402-1406, 1996.
Seward, A. C., Antarctic fossil plants. British Antarctic (Terra Nova) Expedition 1910. *Natural History Reports. Geology, 1 (1)*. London, 1914.
Shaw, R. H., and A. R. Pereira, Aerodynamic roughness of a plant canopy: a numerical experiment, *Ag. Met.*, *26*, 51-65, 1982.
Shugart, H. H., Importance of structure in the longer-term dynamics of landscapes, *J. Geophys. Res.*, *105*, D20065-D20075, 2000.
Shuttleworth, W. J., and J. S. Wallace, Evaporation from sparse crops – an energy combination theory, *Q. J. Roy. Met. Soc.*, *111*, 839-855, 1985.
Sollins, P., C. C. Grier, F. M. McCorison, K. Cromack, R. Fogel, and R. L. Frederiksen, The internal element cycles of an old-growth Douglas-Fir ecosystem in western Oregon, *Ecol. Mon.*, *50*, 261-285, 1980.
Spicer, R. A., and J. L. Chapman, Climate change and the evolution of high-latitude terrestrial vegetation and floras, *Trends Ecol. Evol.*, *5*, 279-284, 1990.
Spicer, R. A., and J. T. Parrish, Palaeobotanical evidence for cool north polar climates in middle Cretaceous (Albanian-Cenomanian) time, *Geology*, *14,* 703-706, 1986.
Spicer, R. A., and J. T. Parrish, Late Cretaceous-early Tertiary palaeoclimates of northern high latitudes: a quantitative view, *J. Geol. Soc., Lond., 147,* 329-341, 1990.
Steele, S. J., S. T. Gower, J. G. Vogel, and J. M. Norman, Root mass, net primary production and turnover in aspen, jack pine, and black spruce forests in Saskatchewan and Manitoba, Canada, *Tree Physiol.*, *17*, 577-587, 1997.
Striegl, R. G., and K. P. Wickland, Effects of a clear-cut harvest on soil respiration in a jack pine-lichen woodland, *Can. J. For. Res., 28,* 534-539, 1998.
Szaniawski, R. K., Growth and maintenance respiration of shoot and roots in Scots Pine seedlings, *Zeit. Pflanzenphysiol.*, *101*, 391-398, 1981.
Tamai, K., T. Abe, M. Araki, and H. Ito, Radiation budget, soil heat flux and latent heat flux at the forest floor in a warm, temperate mixed forest, *Hydrol. Processes*, *12*, 2105-2114, 1998.
Taylor, E. L., T. N. Taylor, and N. R. Cuneo, The present is not the key to the past: a polar forest from the Permian of Antarctica, *Science, 257,* 1675-1677, 1992.
Thomas, S. C., and W. E. Winner, Leaf area index of an old-growth Douglas fir forest estimated from direct structural measurements in the canopy, *Can. J For. Res*., *30*, 1922-1930, 2000.
Thornley, J. H. M., Respiration, growth and maintenance in plants, *Nature*, *227*, 304-305, 1970.
Thornley, J. H. M., Dynamic model of leaf photosynthesis with acclimation to light and nitrogen, *Ann. Bot., 81*, 421-430, 1998.
van Cleve, K., R. Barney, and R. Schlentner, Evidence of temperature control of production and nutrient cycling in two interior Alaska black spruce ecosystems, *Can. J. For. Res.*, *11*, 258-273, 1981.
Vitousek, P. M., and R .W. Howarth, Nitrogen limitation on land and in sea. How can it occur ?, *Biogeochemistry*, *13,* 87-115, 1991.
Vogt, K. A., C. C. Grier, D. J. Vogt, Production, turnover, and nutrient dynamics of above- and below-ground detritus of World forests, *Adv. Ecol. Res. 15,* 303-366 1986.
Vogt, K. A., D. J. Vogt, P. A. Palmiotto, P. Boon, J. O'Hara, and H. Asbjornson, Review of root dynamics in forest ecosystems grouped by climate, climatic forest type and species, *Plant Soil*, *187*, 159-219, 1996.
von Caemmerer, S., *Biochemical Models of Leaf Photosynthesis*. CSIRO Publishing, Melbourne, 2000.

Walcroft, A. S., D. Whitehead, W. B. Silvester, and F. M. Kelliher, The response of photosynthetic model parameters to temperature and nitrogen concentration in *Pinus radiata* D. Don, *Plant Cell Environ.*, *20*, 1338-1348, 1997.

Weiss, A., and J. M. Norman, Partitioning solar radiation into direct and diffuse, visible and near-infrared components, *Ag. For. Met.*, *34*, 205-213, 1985.

Weiss, S. B., Vertical and temporal distribution of insolation in gaps in an old-growth coniferous forest, *Can. J. For. Res., 30*, 1953-1964, 2000.

White A., M.G.R. Cannell, and A.D. Friend, The high-latitude terrestrial carbon sink: a model analysis, *Global Change Biol. 6,* 227-245, 2000.

Williams, E. J., A. Guenther, and S. C. Fehsenfeld, An inventory of nitric oxide emissions from soils in the United States, *J. Geophys. Res.*, *97*, 7511-7519, 1992.

Wilson, K. B., D. D. Baldocchi, and P. J. Hanson, Spatial and seasonal variability of photosynthetic parameters and their relationship to leaf nitrogen in a deciduous forest, *Tree Physiol.*, *20*, 565-578, 2000a.

Wilson, K. B., P. J. Hanson, and D. D. Baldocchi, Factors controlling evaporation and energy partitioning beneath a deciduous forest over an annual cycle, *Ag. For. Met.*, *102*, 83-103, 2000b.

Wirth, C., Schulze, E.-D., W. Schulze, D. von Stünzner-Karbe, W. Ziegler, I. M. Miljukova, A. Sogatchev, A. B. Varlagin, M. Panvyrov, S. Grigoriev, W. Kusnetzova, M. Siry, G. Hardes, R. Zimmermann, and N. N. Vygodskaya, Above-ground biomass and structure of pristine Siberian Scots pine forests as controlled by competition and fire, *Oecologia*, *121*, 66-80, 1999.

Woodward, F. I., *Climate and Plant Distribution*, 174 pp., Cambridge University Press, Cambridge, 1987.

Woodward, F. I., and Osborne, C. P., The representation of root processes in models addressing the responses of vegetation to global change, *New Phytologist, 147,* 223-232, 2000.

Woodward, F. I., and T. M. Smith, Predictions and measurements of the maximum photosynthetic rate, A_{max}, at the global scale, in *Ecophysiology of Photosynthesis, Ecol. Stud.,* vol. 100, edited by E.D. Schulze and M.M. Caldwell, pp. 491-509, Springer-Verlag, New York, 1994a.

Woodward, F. I., and T. M. Smith, Global photosynthesis and stomatal conductance: modeling the controls by soils and climate. *Adv. Bot. Res., 20,* 1-41, 1994b.

Woodward, F.I., T. M. Smith, and W. R. Emanuel, A global land primary productivity and phytogeography model, *Global Biogeochem. Cycles*, *9,* 471-490, 1995.

C.P. Osborne and D.J. Beerling, Department of Animal and Plant Sciences, University of Sheffield, Sheffield S10 2TN, U.K. (e-mail: C.P.Osborne@sheffield.ac.uk, D.J.Beerling@sheffield.ac.uk).

(Received August 10, 2001; revised April 2, 2002;
accepted April 5, 2002.)

Paper number 2001GB001467.
0886-6236/01/2001GB001467$12.00

Paper number 2001GB001467.

Published in 2001 by the American Geophysical Union.

Paper number 2001GB001467.

****Provide running head (45 character max for short title):**

OSBORNE AND BEERLING: MODELING POLAR CONIFER FORESTS

Figure 1. The functional consequences of an increase in leaf lifespan from the leaf to the ecosystem scale, as represented by the model. Numbers indicate the model equations describing leaf-scale relationships. Arrows linking boxes indicate interactions between processes at progressively larger scales. Arrows within boxes denote the direction of change in a process generally resulting from an increase (↑) in leaf lifespan.

Figure 1. The functional consequences of an increase in leaf lifespan from the leaf to the ecosystem scale, as represented by the model. Numbers indicate the model equations describing leaf-scale relationships. Arrows linking boxes indicate interactions between processes at progressively larger scales. Arrows within boxes denote the direction of change in a process generally resulting from an increase (↑) in leaf lifespan.

Figure 2. Schematic of the principal processes represented by the model, and their key interactions. Boxes show biological processes, ovals distinguish data inputs, solid arrows denote matter fluxes, and dotted lines indicate the coupling between processes, with arrowheads showing the direction of influence. The input of solar energy to the system and its important effects are indicated by 'energy balance'.

Figure 2. Schematic of the principal processes represented by the model, and their key interactions. Boxes show biological processes, ovals distinguish data inputs, solid arrows denote matter fluxes, and dotted lines indicate the coupling between processes, with arrowheads showing the direction of influence. The input of solar energy to the system and its important effects are indicated by 'energy balance'.

Figure 3. New model functions, based on field observations of contemporary species. The plotted line in each panel was obtained by fitting model equations to the published data shown as symbols. Equation numbers used in the text and the r^2 for fits are indicated for each. Upper left panel, the dependence of leaf *in vivo* carboxylation capacity V_m on nitrogen content N_l (20) using mean biome observations from *Beerling and Quick* [1995] and *Reich et al*. [1999]. Upper middle panel, the relationship between leaf dark respiration R_m and V_m (23), with mean biome observations from *Reich et al*. [1999]. Upper right panel, the decline in the leaf mass: area ratio M_L with depth into the leaf canopy, as indicated by the overlying leaf area index L (12): circles, *Pinus ponderosa*; squares, *Pseudotsuga menziesii*; triangles, *Tsuga heterophylla* [*Bond et al.*, 1999]. Lower left panel, the correlation between stomatal conductance g_s and net leaf photosynthesis A (34) in thirteen conifer species [*Reich et al*., 1999]. Lower middle panel, the relative decline in canopy stomatal conductance $f(D_a)$ with atmospheric vapour pressure deficit D_a (35) resulting from stomatal closure in *Pinus pinaster* (triangles) and *Picea abies* (circles) canopies [*Granier et al.*, 1996]. Lower right panel, the relative sensitivity of canopy stomatal conductance $f(w_a)$ to soil moisture availability w_a (36), from the model of *Granier and Loustau* [1994], developed for *Pinus pinaster*.

Figure 3. New model functions, based on field observations of contemporary species. The plotted line in each panel was obtained by fitting model equations to the published data shown as symbols. Equation numbers used in the text and the r^2 for fits are indicated for each. Upper left panel, the dependence of leaf *in*

vivo carboxylation capacity V_m on nitrogen content N_l (20) using mean biome observations from *Beerling and Quick* [1995] and *Reich et al*. [1999]. Upper middle panel, the relationship between leaf dark respiration R_m and V_m (23), with mean biome observations from *Reich et al*. [1999]. Upper right panel, the decline in the leaf mass: area ratio M_L with depth into the leaf canopy, as indicated by the overlying leaf area index L (12): circles, *Pinus ponderosa*; squares, *Pseudotsuga menziesii*; triangles, *Tsuga heterophylla* [*Bond et al.*, 1999]. Lower left panel, the correlation between stomatal conductance g_s and net leaf photosynthesis A (34) in thirteen conifer species [*Reich et al*., 1999]. Lower middle panel, the relative decline in canopy stomatal conductance $f(D_a)$ with atmospheric vapour pressure deficit D_a (35) resulting from stomatal closure in *Pinus pinaster* (triangles) and *Picea abies* (circles) canopies [*Granier et al.*, 1996]. Lower right panel, the relative sensitivity of canopy stomatal conductance $f(w_a)$ to soil moisture availability w_a (36), from the model of *Granier and Loustau* [1994], developed for *Pinus pinaster*.

Figure 4. Leaf area index L_a. Upper panel, simulated values are compared to observations in conifer forests from a range of geographical regions, distinguished by different symbols (Table 3). The solid line shows exact agreement, while the dashed line is a regression of simulated values against observations with $r^2 = 0.63$. Lower panel, as upper panel, using a clumping factor value of 0.40 for sites where dominant vegetation is a mixture of *Pseudotsuga menziesii* and *Tsuga heterophylla* (see text for details). Regression is improved so that $r^2 = 0.88$.

Figure 4. Leaf area index L_a. Upper panel, simulated values are compared to observations in conifer forests from a range of geographical regions, distinguished by different symbols (Table 3). The solid line shows exact agreement, while the dashed line is a regression of simulated values against observations with $r^2 = 0.63$. Lower panel, as upper panel, using a clumping factor value of 0.40 for sites where dominant vegetation is a mixture of *Pseudotsuga menziesii* and *Tsuga heterophylla* (see text for details). Regression is improved so that $r^2 = 0.88$.

Figure 5. Net primary productivity P_n. Upper panel, simulated values are compared to observations in conifer forests from a range of geographical regions, distinguished by different symbols (Table 3). The solid line shows exact agreement, while the dashed line is a regression of simulated values against observations with $r^2 = 0.91$. Lower panel, difference between simulated and observed P_n values by region. Positive values indicate overestimation by the model.

Figure 5. Net primary productivity P_n. Upper panel, simulated values are compared to observations in conifer forests from a range of geographical regions, distinguished by different symbols (Table 3). The solid line shows exact agreement, while the dashed line is a regression of simulated values against observations with $r^2 = 0.91$. Lower panel, difference between simulated and observed P_n values by region. Positive values indicate overestimation by the model.

Figure 6. Upper left, middle and right panels, carbon partitioning to leaves P_l, sapwood P_s and roots P_r, respectively. Lower left, middle and right panels, leaf area index L_a; evapotranspiration E; and plant nitrogen consumption, the sum of root nitrogen uptake N_u and re-translocation from senescing leaves N_t, respectively. For each forest type, the simulated and observed (mean ± s.e.) properties are shown for the same, or closely located, sites indicated by asterisks in Table 3.

Figure 6. Upper left, middle and right panels, carbon partitioning to leaves P_l, sapwood P_s and roots P_r, respectively. Lower left, middle and right panels, leaf area index L_a; evapotranspiration E; and plant nitrogen consumption, the sum of root nitrogen uptake N_u and re-translocation from senescing leaves N_t, respectively. For each forest type, the simulated and observed (mean ± s.e.) properties are shown for the same, or closely located, sites indicated by asterisks in Table 3.

Figure 7. Season course of observed (points) and simulated (broken lines) energy partitioning for a boreal forest landscape, dominated by *Picea mariana* in Canada (* site in Table 3).

Observations from *A. L. Dunn, S.C. Wofsy, M.L. Goulden and J.W. Munger* [*unpublished data*].

Figure 7. Season course of observed (points) and simulated (broken lines) energy partitioning for a boreal forest landscape, dominated by *Picea mariana* in Canada (* site in Table 3). Observations from *A. L. Dunn, S.C. Wofsy, M.L. Goulden and J.W. Munger* [*unpublished data*].

Figure 8. Sensitivity of simulated net primary productivity P_n to pCO_2, elevated air temperature and a change in solar energy flux. Results are shown for the four sites used in Figure 6 and three scenarios: 'control', using unmodified climate and soil data inputs; 'warming', with a 4.8°C warming, equivalent to the radiative forcing effect from a rise in C_a from 35 to 100 Pa; 'warming + aerosol', with a 4.8°C warming, 10% reduction in direct and 33% enhancement of diffuse solar radiation. See text for further details.

Figure 8. Sensitivity of simulated net primary productivity P_n to pCO_2, elevated air temperature and a change in solar energy flux. Results are shown for the four sites used in Figure 6 and three scenarios: 'control', using unmodified climate and soil data inputs; 'warming', with a 4.8°C warming, equivalent to the radiative forcing effect from a rise in C_a from 35 to 100 Pa; 'warming + aerosol', with a 4.8°C warming, 10% reduction in direct and 33% enhancement of diffuse solar radiation. See text for further details.

Figure 9. Relationship between CO_2-saturated net primary productivity P_n determined from the 'control' and 'warming' scenarios (Figure 8) and mean annual temperature for the four reference sites. Arrows to broken lines indicate the effects of alleviating constraints on nitrogen uptake rate by decomposition at the Southern US swamp site (see text for details). Values in brackets are leaf lifespan for the dominant species (Table 3).

Figure 9. Relationship between CO_2-saturated net primary productivity P_n determined from the 'control' and 'warming' scenarios (Figure 8) and mean annual temperature for the four reference sites. Arrows to broken lines indicate the effects of alleviating constraints on nitrogen uptake rate by decomposition at the Southern US swamp site (see text for details). Values in brackets are leaf lifespan for the dominant species (Table 3).

Plate 1. Sensitivity of simulated leaf area index (L_a) and net primary productivity (P_n) to leaf lifespan and the geographical variations in climate and soils. Maps are polar projections of model simulations for the northern hemisphere made using climatic data from *New et al.* [1999, 2000] and soils from the *Global Soil Data Task* [2000]. Upper left panel, L_a for a leaf lifespan of 6 months; upper right panel, P_n for a leaf lifespan of 6 months; middle left panel, L_a for a leaf lifespan of 120 months; middle right panel, P_n for a leaf lifespan of 120 months; lower left panel, the difference in L_a between simulations for 6 and 120 months; lower right panel, the difference in P_n between simulations for 6 and 120 months. In the lower panels, positive numbers indicate higher values for the 6 than the 120 month leaf lifespan simulation, while negative numbers indicate lower values.

Plate 1. Sensitivity of simulated leaf area index (L_a) and net primary productivity (P_n) to leaf lifespan and the geographical variations in climate and soils. Maps are polar projections of model simulations for the northern hemisphere made using climatic data from *New et al.* [1999, 2000] and soils from the *Global Soil Data Task* [2000]. Upper left panel, L_a for a leaf lifespan of 6 months; upper right panel, P_n for a leaf lifespan of 6 months; middle left panel, L_a for a leaf lifespan of 120 months; middle right panel, P_n for a leaf lifespan of 120 months; lower left panel, the difference in L_a between simulations for 6 and 120 months; lower right panel, the difference in P_n between simulations for 6 and 120 months. In the lower panels, positive numbers indicate higher values for the 6 than the 120 month leaf lifespan simulation, while negative numbers indicate lower values.

Plate 1. Sensitivity of simulated leaf area index (L_a) and net primary productivity (P_n) to leaf lifespan and the geographical variations in climate and soils. Maps are polar projections of model simulations for the northern hemisphere made using climatic data from *New et al.* [1999, 2000] and soils from the *Global Soil Data Task* [2000]. Upper left panel, L_a for a leaf lifespan of 6 months; upper right panel, P_n for a leaf lifespan of 6 months; middle left panel, L_a for a leaf lifespan of 120 months; middle right panel, P_n for a leaf lifespan of 120 months; lower left panel, the difference in L_a between simulations for 6 and 120 months; lower right panel, the difference in P_n between simulations for 6 and 120 months. In the lower panels, positive numbers indicate higher values for the 6 than the 120 month leaf lifespan simulation, while negative numbers indicate lower values.

Table 1. Treatment of ecosystem physiology in the University of Sheffield Conifer Model (USCM)

Physiology	Treatment
Shortest time step	1 hour
Photosynthesis	enzyme-based [*Farquhar et al.*, 1980], dependent on leaf lifespan
N uptake by vegetation	dependent on soil carbon and nitrogen status, and air temperature [*Woodward et al.*, 1995]
Stomatal conductance	dependent on photosynthesis, leaf-to-air vapor pressure deficit, atmospheric CO_2, soil moisture [*Leuning*, 1995; *Woodward et al.*, 1995]
Radiation	Sunlit and shaded 'big-leaf' canopy absorption of near-infrared and photosynthetically active fractions [*de Pury and Farquhar,* 1997]
Canopy temperature	canopy energy balance [*Monteith and Unsworth*, 1990]
Aerodynamics	dependent on leaf area index and height [*Shaw and Pereira*, 1982]
Sapwood respiration	dependent on sapwood volume and temperature [*Ryan et al.*, 1995]
Fine root respiration	dependent on nitrogen and temperature [*Ryan et al.*, 1996].
Leaf area index	has to satisfy carbon, nitrogen and water constraints
C allocation	annual using functional relationships with carbon, nitrogen and water requirements
N allocation	dependent on leaf lifespan and fixed concentrations for wood and roots
Evapotranspiration	transpiration [*Penman*, 1948; *Monteith*, 1965] + interception [*Woodward*, 1987] + soil evaporation [*Chanzy and Bruckler*, 1993]
Water balance	bucket model with one soil layer
N-mineralization	not explicitly simulated

Table 2. Core constants distinguishing conifers from other woody species. Notation: CH_2O, carbohydrate; DM, dry matter

Constant	Value	Units	Sources
a_1, sensitivity of stomatal conductance to photosynthesis	28	m	see Figure 3
d_1, d_2, empirical descriptors of the stomatal response to atmospheric vapor pressure	1199, 566	d'less	see Figure 3
g_{cut}, leaf cuticular conductance	3	mmol H_2O m^{-2} s^{-1}	*Körner* [1994]
H_r, activation energy for respiration at 293 K	l = 9593	J mol^{-1}	*Walcroft et al*. [1997]
(l, leaves; s, sapwood; r, coarse and ephemeral roots)	s = 42850		*Ryan et al*. [1995]
	r = 54110		*Murty et al*. [1996]
k_M, rate of decrease in leaf mass-to-area with canopy area	9.65	-	see Figure 3
N_s, sapwood nitrogen content	1.8	mg g^{-1} DM	*Ryan* [1991]
N_{er}, ephemeral root nitrogen content	10.0		*Gordon and Jackson* [2000]
N_{cr}, coarse root nitrogen content	3.0		
r_N, nitrogen-based root maintenance respiration rate	0.8	nmol CO_2 mg^{-1} N s^{-1}	*Ryan et al*. [1996]
r_v, volume-based sapwood maintenance respiration rate	15.6	μmol CO_2 m^{-3} s^{-1}	*Ryan et al*. [1996]
s_1, s_2, empirical descriptors of the stomatal response to soil drying	0.016, -4.27	d'less	see Figure 3
s_{min}, relative stomatal conductance in a dry soil	0.05	d'less	*Körner* [1994]
Y_G, growth efficiency	l = 0.63	g DM	*Chung and Barnes* [1977]
(l, leaves; s, sapwood; r, coarse and ephemeral roots)	s = 0.68	g^{-1} CH_2O	*Carey et al*. [1997]
	r = 0.66		*Szaniawski* [1981]
α_p, leaf PAR absorptance	0.90	d'less	*Gates* [1979]
α_n, leaf NIR absorptance	0.10	d'less	*Gates* [1979]
φ_r, ephemeral fraction of roots	0.25	d'less	*Vogt et al*. [1996]
Ω, canopy clumping factor	0.55	d'less	*Chen* [1996]
			Chen and Black [1991]
			Chen et al. [1991]
			Fassnacht et al. [1994]
			Weiss [2000]

Table 3. Sites used in model testing, with details for each of its geographical location, latitude, forest type, dominant species, leaf lifespan (Z_l), and observations of leaf area index (L_a) and net primary productivity (P_n) with literature sources. Climatic and soils data inputs are summarized by mean annual temperature (MAT), mean annual precipitation (MAP), soil carbon and nitrogen contents for each. n/a = data not available

Location	Lat. Lon.	Climate regime	Dominant species	Z_l (mths)	MAT (ºC)	MAP (mm)	Soil C[b] (g m^{-2})	Soil N[b] (g m^{-2})	P_n[c] (g C m^{-2} yr^{-1})	L_a[d] (m^2 m^{-2})	Literature sources
Siberia[a]	64°N 100°E	boreal	*Larix gmelinii*	4	-7.3	443	10900	638	83^T	n/a	*Kajimoto et al*. [1999]
Siberia[a]	61°N 128°E	boreal	*L. gmelinii*	4	-8.9	399	10900	638	104^A	2.0^A	*Schulze et al.* [1995]; *Kelliher et al*. [1997]
Siberia	61°N 128°E	boreal	*Pinus sylvestris*	84	-3.7	493	2000	150	149^T	2.4^A	*Schulze et al.* [1999]; *Wirth et al*. [1999]
Alaska	65°N 148°W	boreal	*Picea mariana*	132	-2.4	304	11000	735	220^T	n/a	*McGuire et al*. [1992]
Alaska	64°N 148°W	boreal	*P. mariana*	132	-5.4	283	11000	735	49^A	n/a	*van Cleve et al*. [1981]
Canada[a]	56°N 98°W	boreal	*P. mariana*	138	-1.9	501	15000	980	243^T	4.1^A	*Gower et al.* [1997]; *Steele et al.* [1997]; *Dunn et al.* [unpublished data]
Canada	56°N 99°W	boreal	*Pinus banksiana*	90	-1.7	479	2000	150	293^T	2.2^A	*Gower et al.* [1997]; *Steele et al*. [1997]
Canada	54°N 105°W	boreal	*P. mariana*	132	0.3	432	15000	980	218^T	4.5^A	*Gower et al.* [1997]; *Steele et al*. [1997]
Canada	54°N 105°W	boreal	*P. banksiana*	66	0.4	424	2000	150	237^T	2.5^A	*Gower et al.* [1997]; *Steele et al*. [1997]
Germany	50°N 12°E	cool temperate	*Picea abies*	132	9.1	671	12100	626	518^T	5.0^A	*Schulze et al.* [1999]
Pacific NW	45°N 124°W	cool temperate	*Picea sitchensis*	48	10.2	1581	24000	1210	669^T	5.3^A	*Gholz* [1982]; *Runyon et al*. [1994]
Pacific NW[a]	45°N 123°W	cool temperate	*Pseudotsuga menziesii*	36	11.2	1095	24000	1210	737^T	6.0^A	*Gholz* [1982]; *Runyon et al.* [1994]
Pacific NW[a]	45°N 122°W	cool temperate	*P. menziesii*	36	9.0	2300	24000	1210	n/a	8.6^A	*Thomas and Winner* [2000]; *Chen et al*. [2001]
Pacific NW[a]	44°N 122°W	cool temperate	*P. menziesii*	36	7.3	1604	24000	1210	530^T	n/a	*Grier and Logan* [1977]; *Sollins et al*. [1980]
Pacific NW	45°N 123°W	cool temperate	*Tsuga heterophylla*	36	11.0	1411	24000	1210	1077^T	8.7^A	*Runyon et al.* [1994]
France	45°N 1°W	mediterranean	*Pinus pinaster*	48	12.8	955	8300	645	n/a	6.0^A	*Granier and Loustou* [1994]
France	44°N 1°W	mediterranean	*P. pinaster*	48	13.1	902	8300	645	n/a	3.5^E	*Bruniquel-Pinel and Gatellu-Etchegorry* [1998]
France	43°N 5°E	mediterranean	*Pinus pinea*	24	14.1	931	4150	322	688^T	n/a	*Rapp and Cabanettes* [1981]
Israel	32°N 35°E	mediterranean	*Pinus halepensis*	36	19.4	576	8300	645	n/a	2.5^E	*Schiller and Cohen* [1995]
Southern US	36°N 79°W	warm temperate	*Pinus taeda*	30	15.7	1247	2558	147	1521^T	3.7^E	*Kinerson et al*. [1977]; *Katul et al*. [1999]
Southern US[a]	36°N 76°W	warm temperate	*Taxodium distichum*	6	15.8	1279	15000	1600	999^T	n/a	*Megonigal and Day* [1988]
Southern US[a]	31°N 82°W	warm temperate	*T. distichum*	6	20.0	1260	15000	1600	269^A	2.4^E	*Schlesinger* [1978]; *Liu et al*. [1998]
Southern US	30°N 90°W	warm temperate	*T. distichum*	6	20.4	1561	15000	1600	539^A	n/a	*Connor and Day* [1976]

[a]reference sites used in Figures 6-9. Where more than one location is listed for a given type of forest, we used data from the additional sources given for nearby sites.
[b]soil carbon and nitrogen data from *Woodward and Smith* [1994b] or *Gower et al*. [1997, 2000].
[c]productivity values either: ^{A} above-ground growth; or ^{T} total production.

[d]leaf area indices either: [A] actual (L_a) determined by destructive or allometric methods; or [E] effective (L_e) determined by an optical method.

figure 1

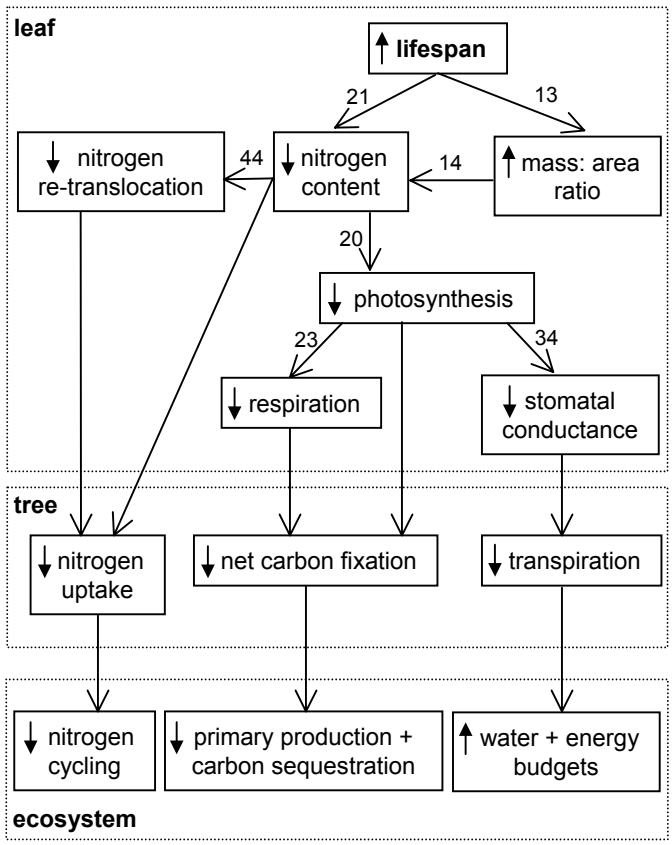
leaf
lifespan
21
13
nitrogen re-translocation
44
nitrogen content
14
mass: area ratio
20
photosynthesis
23
34
respiration
stomatal conductance
tree
nitrogen uptake
net carbon fixation
transpiration
nitrogen cycling
primary production + carbon sequestration
water + energy budgets
ecosystem

figure 2

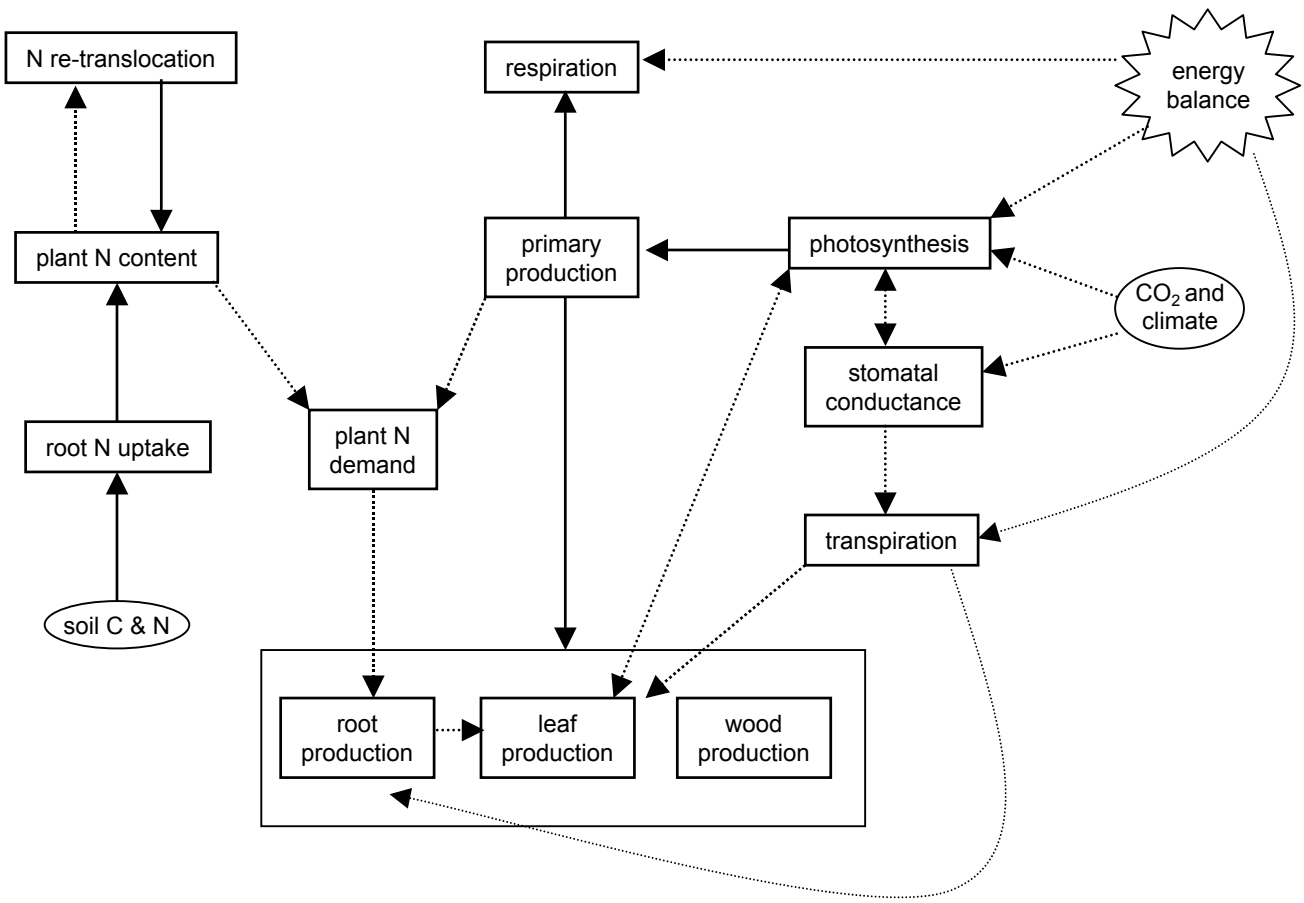
N re-translocation
respiration
energy balance
plant N content
primary production
photosynthesis
CO_2 and climate
stomatal conductance
root N uptake
plant N demand
transpiration
soil C & N
root production
leaf production
wood production

figure 3

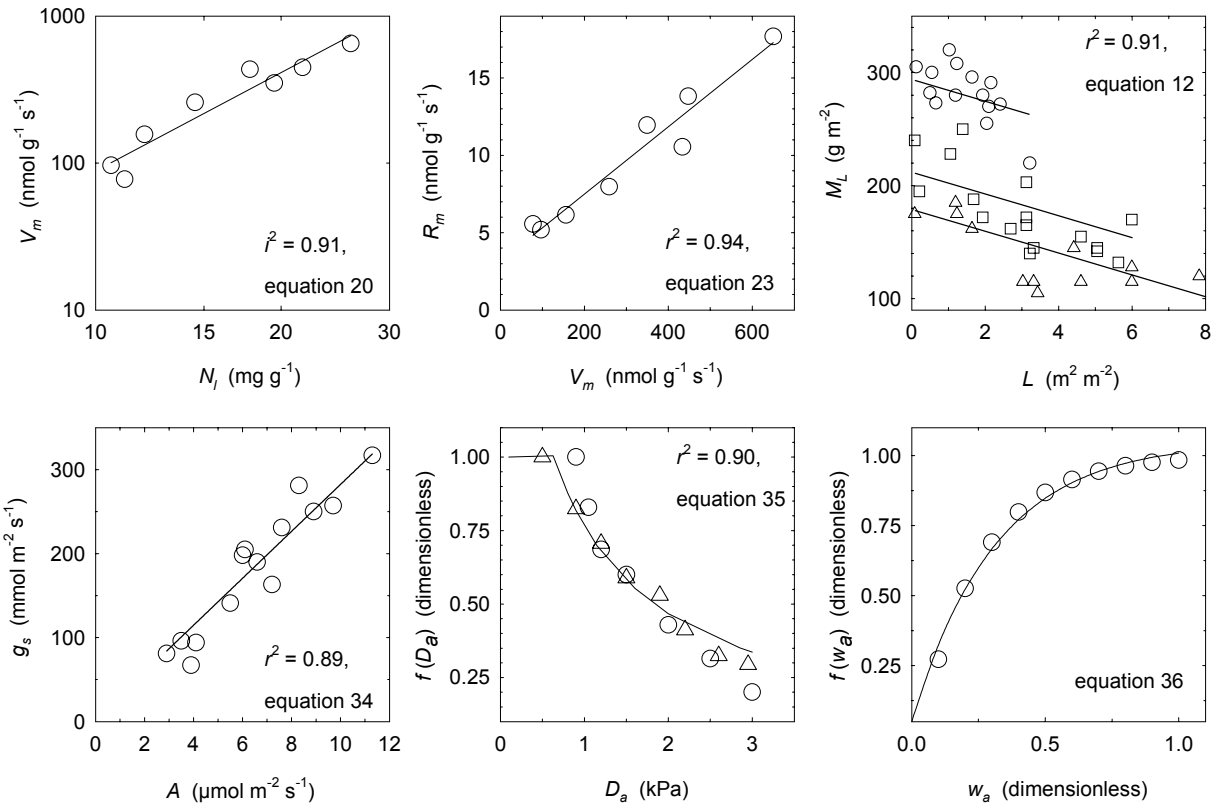
1000
100
10
V_m (nmol g^{-1} s^{-1})
r^2 = 0.91,
equation 20
10
15
20
30
N_l (mg g^{-1})
15
10
5
0
R_m (nmol g^{-1} s^{-1})
r^2 = 0.94,
equation 23
0
200
400
600
V_m (nmol g^{-1} s^{-1})
300
200
100
M_L (g m^{-2})
r^2 = 0.91,
equation 12
0
2
4
6
8
L (m^2 m^{-2})
300
200
100
0
g_s (mmol m^{-2} s^{-1})
r^2 = 0.89,
equation 34
0
2
4
6
8
10
12
A (µmol m^{-2} s^{-1})
1.00
0.75
0.50
0.25
$f(D_a)$ (dimensionless)
r^2 = 0.90,
equation 35
0
1
2
3
D_a (kPa)
1.00
0.75
0.50
0.25
$f(w_a)$ (dimensionless)
equation 36
0.0
0.5
1.0
w_a (dimensionless)

figure 4

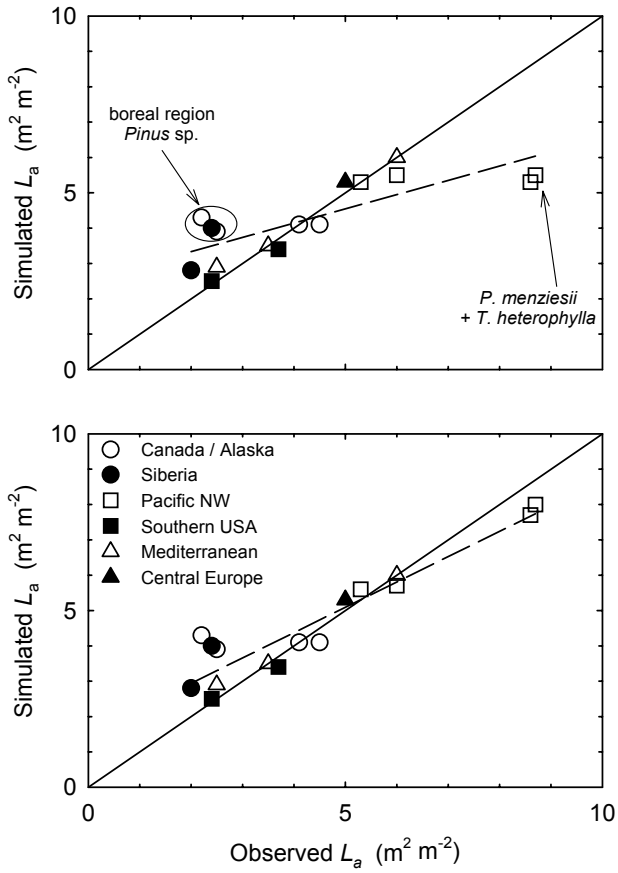
boreal region
Pinus sp.
P. menziesii
+ *T. heterophylla*
Canada / Alaska
Siberia
Pacific NW
Southern USA
Mediterranean
Central Europe
Simulated L_a (m^2 m^{-2})
Observed L_a (m^2 m^{-2})
0
5
10

figure 5

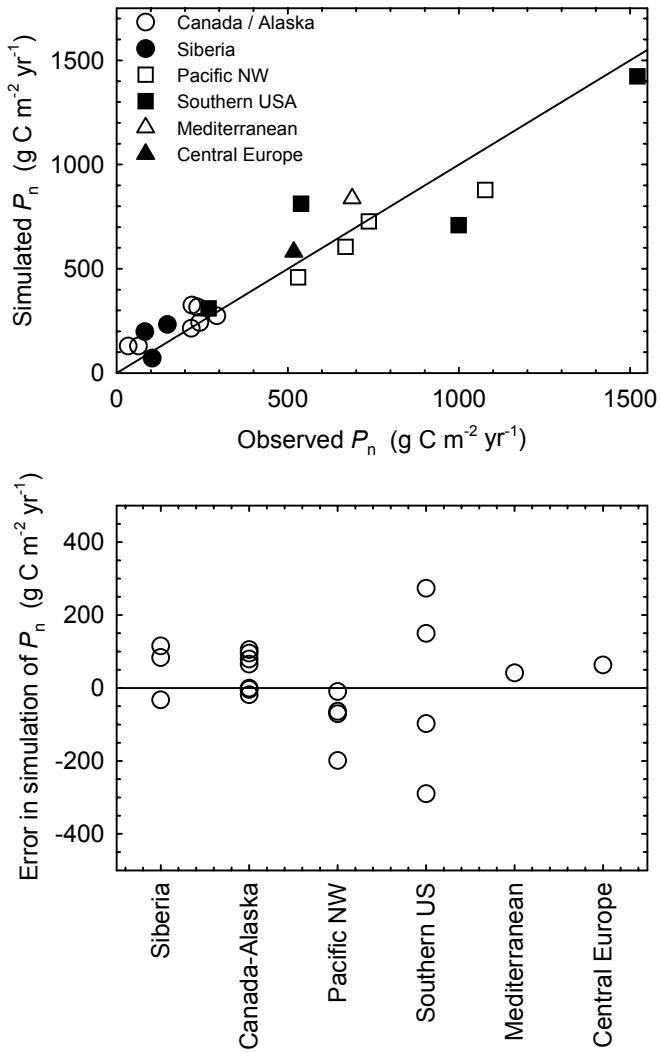
Canada / Alaska
Siberia
Pacific NW
Southern USA
Mediterranean
Central Europe
Simulated P_n (g C m^{-2} yr^{-1})
Observed P_n (g C m^{-2} yr^{-1})
0
500
1000
1500
Error in simulation of P_n (g C m^{-2} yr^{-1})
400
200
0
-200
-400
Siberia
Canada-Alaska
Pacific NW
Southern US
Mediterranean
Central Europe

figure 6

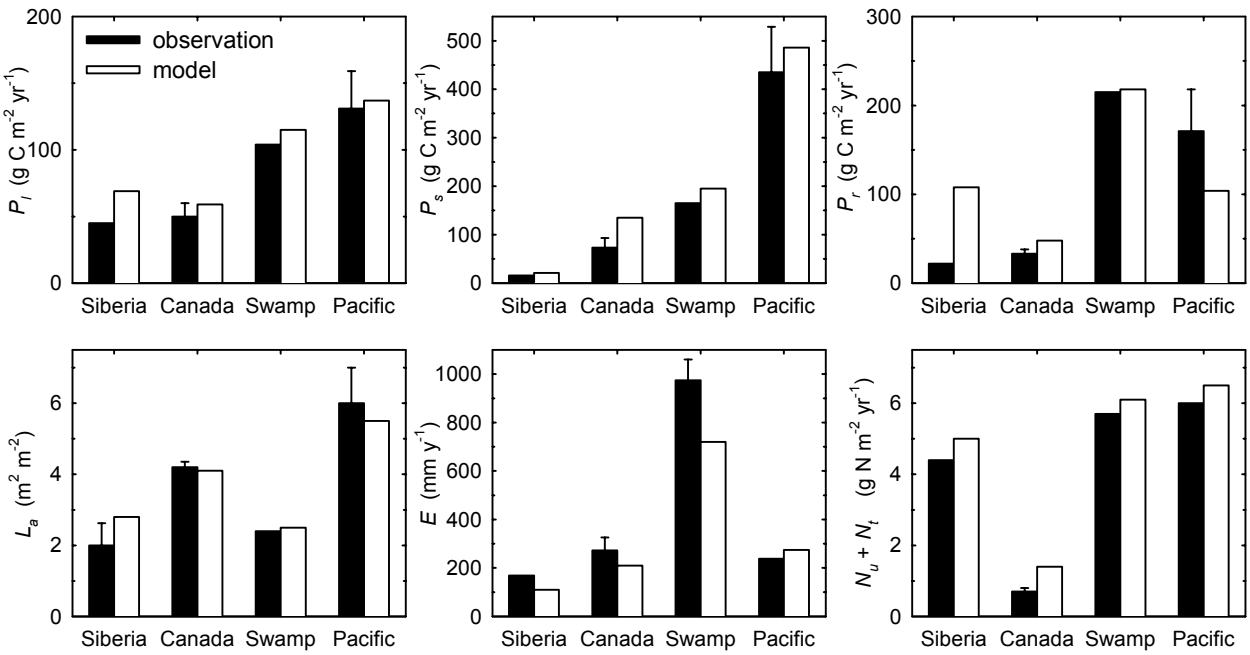
observation
model
P_l (g C m^{-2} yr^{-1})
P_s (g C m^{-2} yr^{-1})
P_r (g C m^{-2} yr^{-1})
L_a (m^2 m^{-2})
E (mm y^{-1})
$N_u + N_t$ (g N m^{-2} yr^{-1})
Siberia
Canada
Swamp
Pacific

figure 7

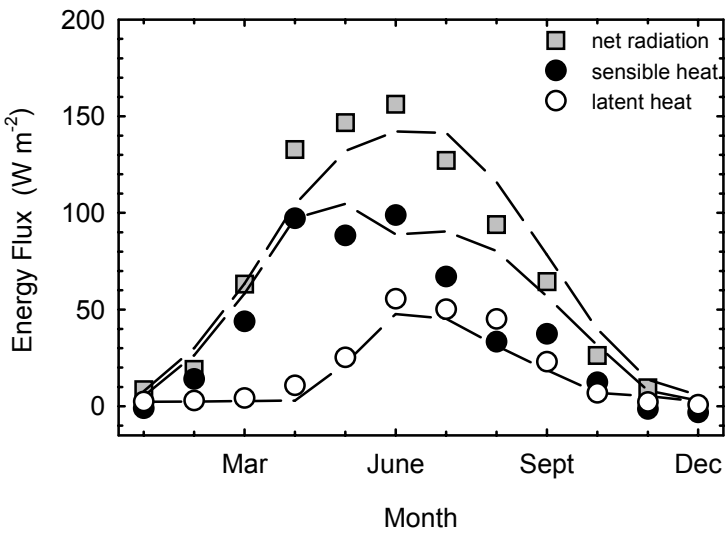
200
150
100
50
0
Energy Flux (W m-2)
net radiation
sensible heat
latent heat
Mar
June
Sept
Dec
Month

figure 8

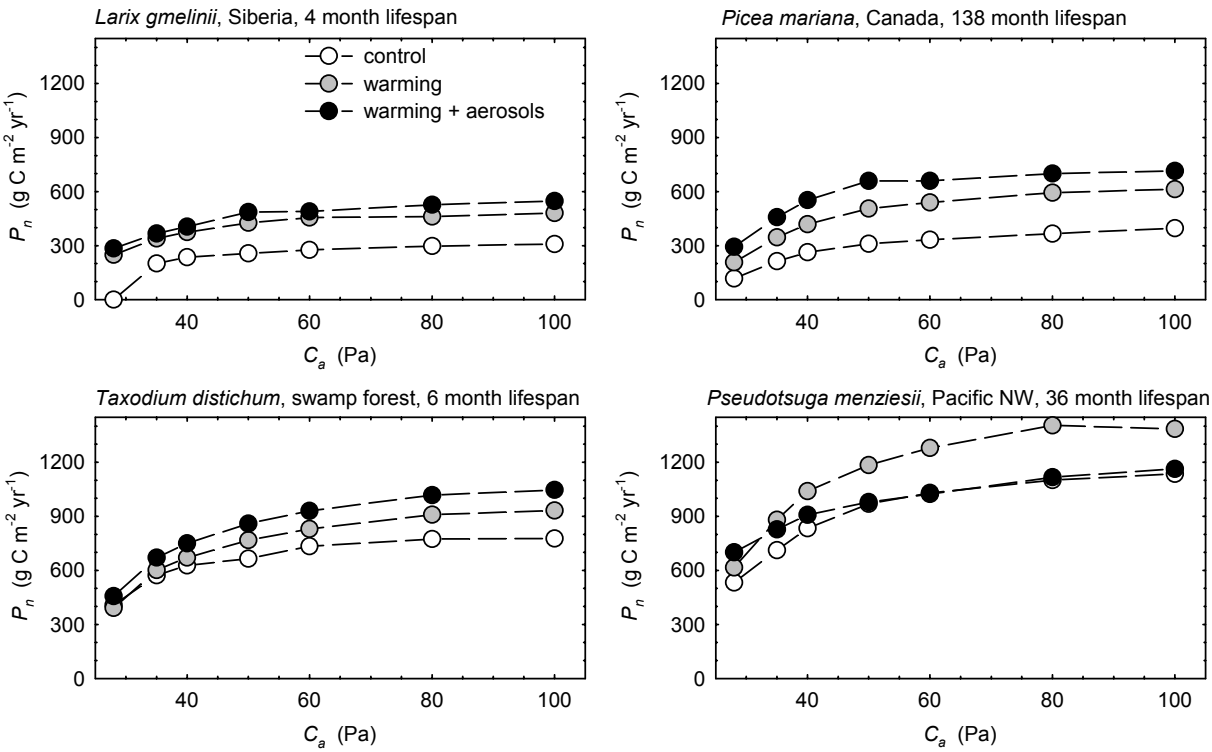
Larix gmelinii, Siberia, 4 month lifespan
control
warming
warming + aerosols
Picea mariana, Canada, 138 month lifespan
Taxodium distichum, swamp forest, 6 month lifespan
Pseudotsuga menziesii, Pacific NW, 36 month lifespan
P_n (g C m^{-2} yr^{-1})
C_a (Pa)
0
300
600
900
1200
40
60
80
100

figure 9

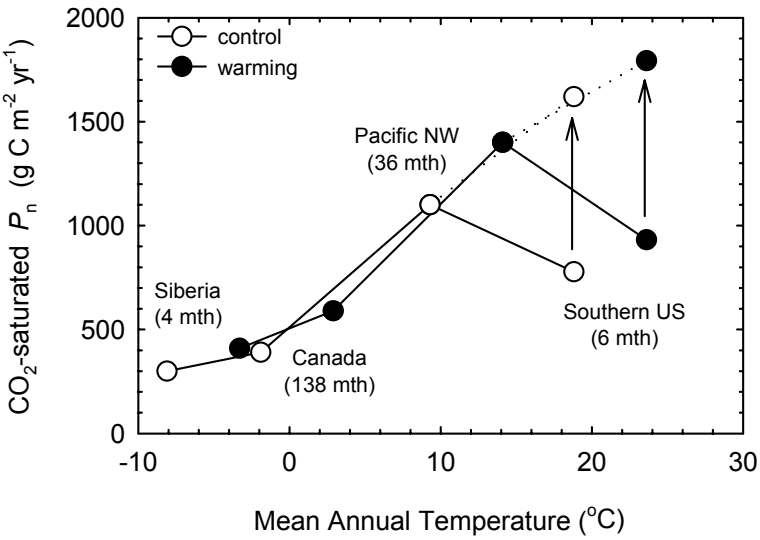
control
warming
Pacific NW
(36 mth)
Siberia
(4 mth)
Canada
(138 mth)
Southern US
(6 mth)
CO_2-saturated P_n (g C m^{-2} yr^{-1})
Mean Annual Temperature (^oC)
2000
1500
1000
500
0
-10
0
10
20
30

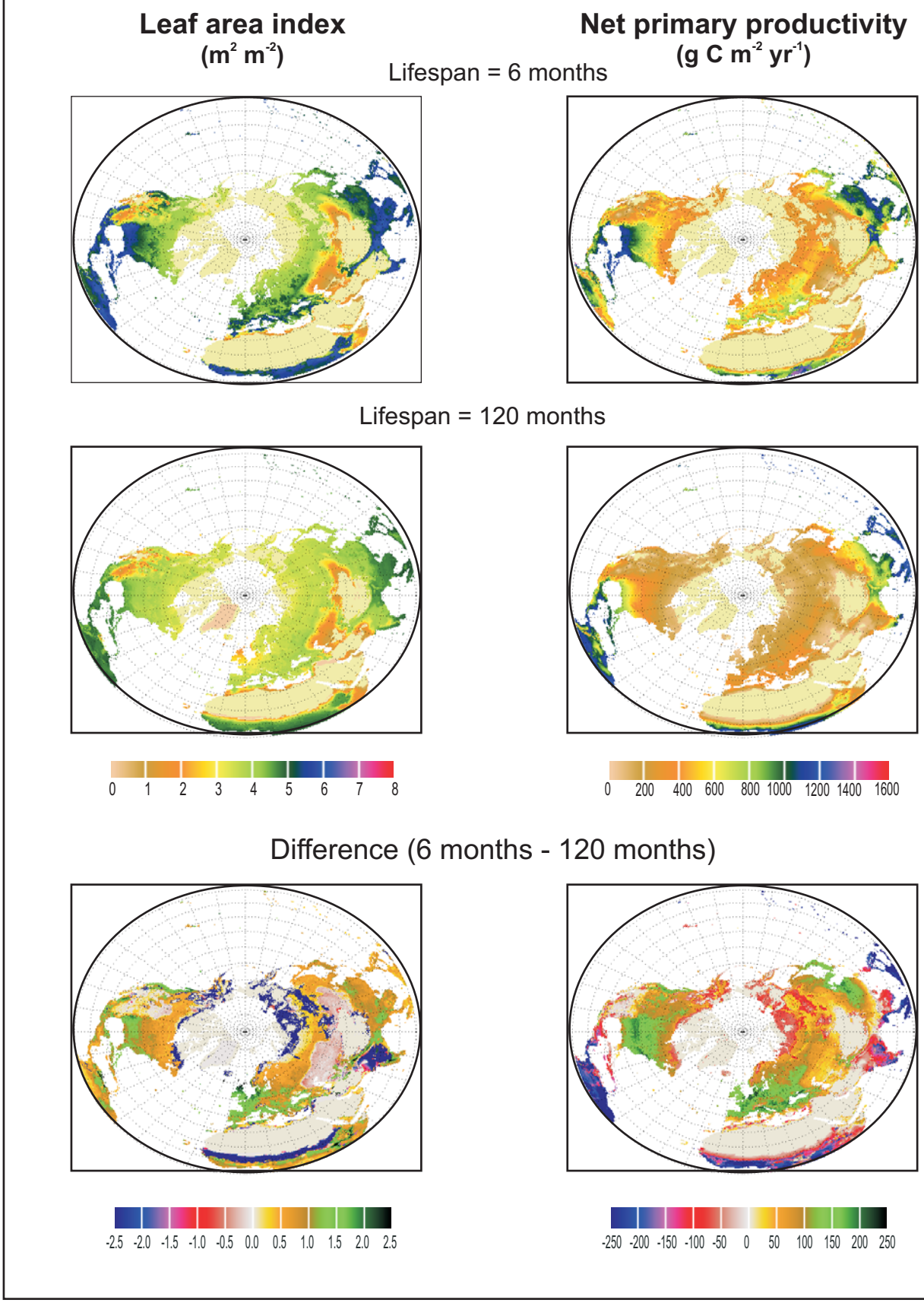
Leaf area index
(m2 m-2)
Net primary productivity
(g C m-2 yr-1)
Lifespan = 6 months
Lifespan = 120 months
0 1 2 3 4 5 6 7 8
0 200 400 600 800 1000 1200 1400 1600
Difference (6 months - 120 months)
-2.5 -2.0 -1.5 -1.0 -0.5 0.0 0.5 1.0 1.5 2.0 2.5
-250 -200 -150 -100 -50 0 50 100 150 200 250